CHARACTERIZATION OF NATURALLY OCCURRING SEVERE COMBINED IMMUNODEFICIENCY (SCID) IN A LINE OF PIGS AND THEIR RESPONSE TO PORCINE REPRODUCTIVE AND RESPIRATORY SYNDROME VIRUS (PRRSV) INFECTION

by

ADA GISELLE CINO-OZUNA

DVM, National University of Asuncion, Paraguay, 2009

AN ABSTRACT OF A DISSERTATION

submitted in partial fulfillment of the requirements for the degree

DOCTOR OF PHILOSOPHY

Department of Diagnostic Medicine/Pathobiology
College of Veterinary Medicine

KANSAS STATE UNIVERSITY
Manhattan, Kansas

2016

Abstract

Severe combined immunodeficiency (SCID) is a rare group of inherited disorders characterized by defects in both humoral and cellular immune functions. Naturally occurring SCID has been first described in humans in the 1960s and subsequently identified in horses, mice, and dogs, but never before in pigs. Affected animals are characterized by having loss of functional B and T lymphocytes, and in some cases natural killer (NK) cells, but normal numbers of monocytes, granulocytes, and megakaryocytes. As a result, affected animals fail to produce antibodies and succumb to common disease pathogens after circulating maternal antibodies decay. SCID models are extremely valuable for the understanding of molecular mechanisms of immunological processes during viral and bacterial diseases, cancer, and autoimmunity. SCID mice are widely used as the current model; however, the relevance of the murine SCID model to human and veterinary immune research is limited and there is an increasing need for a more representative model of SCID is imperative. We describe the gross, microscopic, and immunophenotypic characteristics of a line of Yorkshire pigs having naturally occurring SCID. Affected pigs lack T and B lymphocytes, but display circulating NK cells, fail to produce antibodies to viral infection, and lack cell-mediated response to tumor xenotransplants. We also describe response of SCID pigs to porcine reproductive and respiratory syndrome virus (PRRSV). PRRSV is the most devastating virus in swine industry, causing losses of billions of dollars annually. Understanding the immunopathogenesis of the disease is imperative in order to develop strategies to combat this devastating virus. PRRSV infected-SCID pigs failed to develop lesions of PRRSV infection, demonstrating the significant role of the adaptive immunity to PRRSV infection. Finally, we describe the preliminary results of the adoptive transfer of purified $CD3^+$ T lymphocytes to SCID pigs from SLA-II matched wild-type littermates, with the

objective of establishing a porcine model for the study of T cell immunopathogenesis with viral diseases.

CHARACTERIZATION OF NATURALLY OCCURRING SEVERE COMBINED IMMUNODEFICIENCY (SCID) IN A LINE OF PIGS AND THEIR RESPONSE TO PORCINE REPRODUCTIVE AND RESPIRATORY SYNDROME VIRUS (PRRSV) INFECTION

by

ADA GISELLE CINO-OZUNA

DVM, National University of Asuncion, Paraguay, 2009

A DISSERTATION

submitted in partial fulfillment of the requirements for the degree

DOCTOR OF PHILOSOPHY

Department of Diagnostic Medicine/Pathobiology
College of Veterinary Medicine

KANSAS STATE UNIVERSITY
Manhattan, Kansas

2016

Approved by:

Major Professor
Raymond R. R. Rowland

Copyright

Abstract

Severe combined immunodeficiency (SCID) is a rare group of inherited disorders characterized by defects in both humoral and cellular immune functions. Naturally occurring SCID has been first described in humans in the 1960s and subsequently identified in horses, mice, and dogs, but never before in pigs. Affected animals are characterized by having loss of functional B and T lymphocytes, and in some cases natural killer (NK) cells, but normal numbers of monocytes, granulocytes, and megakaryocytes. As a result, affected animals fail to produce antibodies and succumb to common disease pathogens after circulating maternal antibodies decay. SCID models are extremely valuable for the understanding of molecular mechanisms of immunological processes during viral and bacterial diseases, cancer, and autoimmunity. SCID mice are widely used as the current model; however, the relevance of the murine SCID model to human and veterinary immune research is limited and there is an increasing need for a more representative model of SCID is imperative. We describe the gross, microscopic, and immunophenotypic characteristics of a line of Yorkshire pigs having naturally occurring SCID. Affected pigs lack T and B lymphocytes, but display circulating NK cells, fail to produce antibodies to viral infection, and lack cell-mediated response to tumor xenotransplants. We also describe response of SCID pigs to porcine reproductive and respiratory syndrome virus (PRRSV). PRRSV is the most devastating virus in swine industry, causing losses of billions of dollars annually. Understanding the immunopathogenesis of the disease is imperative in order to develop strategies to combat this devastating virus. PRRSV infected-SCID pigs failed to develop lesions of PRRSV infection, demonstrating the significant role of the adaptive immunity to PRRSV infection. Finally, we describe the preliminary results of the adoptive transfer of purified $CD3^+$ T lymphocytes to SCID pigs from SLA-II matched wild-type littermates, with the

objective of establishing a porcine model for the study of T cell immunopathogenesis with viral diseases.

Table of Contents

List of Figures

List of Tables

Acknowledgements

A journey starts with the first step. I would have never imagined that my first steps in fulfilling my dream of obtaining my PhD would have started in the US. This would have never been possible without the presence and help of **God**. Thank you, Lord, for guiding my very steps and for reminding me of your infinitive love in every aspect of my life.

The long path of earning a doctorate degree certainly cannot be walked alone. I would like to give my immeasurable appreciation to my major professor, **Bob Rowland**, for his advice, encouragement, support, and guidance throughout all of these years. I also would like to thank the members of my committee: **Derek Mosier**, **Walter Renberg**, and **Melinda Wilkerson**, for sharing their knowledge with me and giving me their support.

To all the wonderful people that crossed paths with me during this journey. The **faculty**, **staff**, and **student workers** at Rowland's lab, Immunology lab, LARC, and throughout Mosier Hall. Thank you for all your help and for leaving me with such good memories, experiences, and love.

A huge thank you to my wonderful **friends** in the US, for helping me find a piece of home so far from home. And to my friends in Paraguay, for sending their love and support all the way from the south.

Finally, thank you to my amazing **mom** and **dad**, for supporting and guiding every step of this voyage, for giving me courage when I needed it the most, and for being there when there were hesitations, stumbles, and unexpected turns.

Thank you all! I am very excited to discover where this path would lead me now...

Dedication

To God. You continue to amaze me every day.

To my family here and on Heaven: Ada, Esteban, and Adrian.

Chapter 1 - An introduction to Severe Combined Immunodeficiency Syndrome (SCID)

1.A. Immunodeficiency syndromes

Immunodeficiency is by definition the inability of the immune system to fight against infectious pathogens or the development of cancer (Tizard 2004, Zachary and McGavin, 2012). Immunodeficiencies can be congenital (primary) or acquired (secondary). By far, the most common causes of acquired immunodeficiencies are viral and bacterial infections, and a well-known example is the immunesuppresion caused by infections with the human immunodeficiency virus (HIV). However, other factors such as chemotherapy, autoimmune disease, malnutrition, irradiation, can trigger acquired immunodeficiency.

Primary immunodeficiencies result from inherited or congenital disorders in any of the components of the innate immunity (i.e. lack of completement factors, defects in granules of neutrophils and NK cells, etc.) or the adaptive immune system (i.e. humoral – B cells only, cell-mediated – T cells only, or both). In this dissertation, we will focus on a group of disorders that affect the adaptive immune responses, causing deficiency in both the humoral and cell-mediated arms of the immune system. This group of disorders are collectively called severe combined immunodeficiency (SCID) syndrome.

1.B. Naturally occurring severe combined immunodeficiency (SCID) syndrome

Severe Combined Immunodeficiency (SCID) is a primary immunodeficiency that involves defects in both humoral and cellular immune functions. Because of the absence of cells of the adaptive immunity, affected individuals are incapable of mounting a cell-mediated response and cannot generate an antigen-specific antibodies (Bosma and Carroll 1991, McGuire and Poppie 1973, Perryman 2004, Tedde et al 1980). Naturally occurring SCID was described in mice, horses, dogs, and humans, but was never before reported in pigs. The first reports of SCID in children date back to the 1960s, when affected individuals would die soon after maternal antibody decay due to the inability to mount an immune response to common pathogens (Bauer *et al.* 2009, Meek *et al.* 2009, Perryman 2004).

SCID can result from molecular defects in a variety of proteins required for lymphocyte maturation and/or signal transduction. The most common patterns of inheritance of SCID in veterinary species include autosomal recessive, X-linked, or sporadic, depending on the specific mutation (Bauer *et al.* 2009, Danska *et al.* 1996, Meek *et al.* 2001, Meek *et al.* 2009, Perryman 2004). In autosomal recessive mode of inheritance, affected individuals must carry two copies of the mutated gene (homozygous) to develop the phenotypic disease. Individuals with only one copy of the gene (heterozygous) do not develop the condition. Thus, approximately 25% of the offspring that comes from the mating of heterozygous parents would develop the disease. This is the most common mode of inheritance in animal species. Autosomal recessive inheritance of germline mutations in the catalytic subunit of DNA-dependent protein kinase catalytic subunit (DNA-PKcs) has been identified to cause SCID in C.B-17 mice, Arabian foals, and Jack Russell terrier dogs.

X-linked refers to a mode of inheritance of mutations in the X chromosome. The most common X-linked SCID (XSCID) is caused by defects in the gamma chain of the interleukin-2 receptor (IL-2R) and affects the Bassett Hound and Cardigan Welsh Corgi dogs (Bauer *et al.* 2009, Bell *et al.* 2002, Blunt *et al.* 1995, Bosma and Carroll 1991, Meek *et al.* 2001, Meek *et al.* 2009, Perryman 2004).

The best-studied model of SCID is the murine C.B-17 SCID model. These animals are characterized by severe leukopenia due to prominent lymphopenia, and serum Ig concentrations of less than 0.02 mg/ml due to absence of the major serum isotypes (lgM, IgG3, IgGl, IgG2b, IgG2a, and IgA) (Bosma and Carroll 1991, Custer *et al.* 1985). Except for bone marrow, which appears histologically normal, all lymphoid tissues and organs are hypoplastic (Bosma and Carroll 1991, Custer et al 1985) in C-B-17 mice. The thymus is often grossly undetectable and is microscopically composed of unorganized fibrocollagenous stroma with total absence of lymphocytes and corticomedullary delineation (Bosma and Carroll 1991, Custer *et al.* 1985). Lymph nodes contain few identifiable lymphocytes, but are recognized from their basic stromal structure and sinus pattern. In the spleen, lymphoid follicles and germinal centers are replaced by stromal cell elements, fibroblasts and macrophages (Bosma and Carroll 1991, Custer *et al.* 1985). Some of these C.B.-17 SCID mice preserve the ability to produce very small amounts of immunoglobulin and possess low numbers of mature T lymphocytes and are called "leaky SCID", and has been only described in mice (Bosma *et al.* 1988).

SCID Arabian foals, as well as affected Jack Russell Terriers share similar gross and microscopic features as described in C.B.-17 SCID mice (Bell *et al.* 2002, Bosma and Carroll 1991, Lunn *et al.* 1995, McGuire and Poppie 1973, Meek *et al.* 2001). However, SCID Arabian foals and Jack Russell Terrier dogs also exhibit normal numbers and function of monocytes,

granulocytes, megakaryocytes, erythrocytes, and NK cells (Bosma and Carroll 1991, Custer *et al*. 1985, Lunn *et al.* 1995).

This dissertation describes the phenotypic characteristic of naturally occurring SCID in pigs and their ability to respond to infection with porcine reproductive and respiratory syndrome virus (PRRSV). It also describes the first engraftment of purified $CD3^+$ thymocytes from donor wild type (WT) pigs into SLA II-matched receptor SCID littermates and the different immunophenotypes of T cells present in the receptor SCID pigs, with the hope of establishing an animal model for the study of cell-mediated adaptive immunity during infectious diseases, autoimmunity, and cancer.

1.C. References

1. Basel, M.T., Balivada, S., Beck, A.P., Kerrigan, M.A., Pyle, M.M., Wyatt, C.R., Rowland, R.R.R., Anderson, D.E., Troyer, D.L. (2012). Human xenografts are not rejected in a naturally occurring immunodeficient porcine line: a human tumor model in pigs. *Biores. Open Access* 1, 63–68.

2. Bauer, T.R., Adler, R.L., and Hickstein, D.D. (2009). Potential Large Animal Models for Gene Therapy of Human Genetic Diseases of Immune and Blood Cell Systems. *ILAR J.* 50(2):168-186.

3. Bell, T.G., Butler, K.L., Sill, H.B et al. (2002). Autosomal recessive severe combined immunodeficiency of Jack Russell Terriers. *J Vet Diagn Invest*. 14:194-204.

4. Blunt T, Finnie NJ, Taccioli GE et al. (1995). Defective DNA-Dependent Protein Kinase Activity is Linked to V(D)J Recombination and DNA Repair Defects Associated with the Murine scid Mutation. *Cell.* 80:813-823.

5. Bosma GC, Fried M, Custer RP, et al. (1988). T Evidence of functional lymphocytes in some (leaky) scid mice. *J Experim Med*. 167(3):1016-1033.

6. Bosma MJ and Carroll AM. (1991). The SCID Mouse Mutant: Definition, Characterization and Potential Uses. *Ann Rev Immunol*. 9:323-330.

7. Cino-Ozuna, A.G., Rowland, R.R.R., Nietfeld, J.C., Kerrigan, M.A., Dekkers,J.C., Wyatt, C.R. (2013). Preliminary findings of a previously unrecognized porcine primary immunodeficiency disorder. *Vet. Pathol.* 50,144–146.

8. Custer R.P., Bosma G.C. and Bosma M.J. (1985). Severe Combined Immunodeficiency (SCID) in the Mouse. Pathology, Reconstitution, Neoplasms. *Am J Pathol*. 120:464-477.

9. Danska JS, Holland DP, Mariathasan S et al. (1996). Biochemical and Genetic Defects in the DNA-Dependent Protein Kinase in Murine scid Lymphocytes. *Mol Cell Biol.* 16(10):5507-5517.

10. Lunn DP, McClure JT, Schobert CS et al. (1995). Abnormal patterns of equine leukocyte differentiation antigen expression in severe combined immunodeficiency foals suggests the phenotype of normal equine natural killer cells. *Immunology.* 84:495-499.

11. Zachary JF and McGavin MD. (2012). Pathologic Basis of Veterinary Disease. Chapter 5: Diseases of Immunity. 5th ed.:Elsevier-Mosby, St. Louis, Missouri.

12. McGuire, TC and Poppie, M.J. (1973). Hypogammaglobulinemia and Thymic Hypoplasia in Horses: a Primary Combined Immunodeficiency Disorder. *Infection and Immunity*. 8(2):272-277.

13. Meek K, Jutkowitz A, Allen L et al. (2009). SCID Dogs: Similar Transplant Potential but Distinct Intra-Uterine Growth Defects and Premature Replicative Senescence Compared with SCID Mice. *J Immunol*. 183:2529-2536.

14. Meek K, Kienker L, Dallas C et al. (2001). SCID in Jack Russell Terriers: A New Animal Model of DNA-PKcs Deficiency. *J Immunol*. 167:2142-2150.

15. Perryman LE. (2004). Molecular Pathology of Severe Combined Immunodeficiency in Mice, Horses, and Dogs. *Vet Pathol*. 41:95-100.

16. Tedde A, Balkis ME, Ikehara S et al. (1980). Animal model for immune dysfunction associated with adenosine deaminase deficiency. *Proc Natl Acad Sci*. 77(8):4899-4903.

17. Tizard, I.R. (2004). Veterinary Immunology. Chapter 35: Primary Immunodeficiencies. 7th ed: Elsevier.

Chapter 2 - Preliminary findings of a previously unrecognized porcine primary immunodeficiency disorder

Ada Giselle Cino-Ozuna[1], Raymond R. R. Rowland[1], Jerome C. Nietfeld[1], Maureen A. Kerrigan[1], Jack C. M. Dekkers[2], and Carol R. Wyatt[1]

[1] Department of Diagnostic Medicine/Pathobiology, Kansas State University, Manhattan, KS 66506, United States

[2] Department of Animal Science, Iowa State University, Ames, IA 50011, United States

Abstract

Weaned pigs from a line bred for increased feed efficiency were enrolled in a study of the role of host genes in the response to infection with Porcine Reproductive and Respiratory Syndrome Virus (PRRSV). Four of the pigs were euthanatized early in the study due to weight loss with illness and poor body condition; 2 pigs before PRRSV infection and the other 2 pigs approximately 2 weeks after virus inoculation. The 2 inoculated pigs failed to produce PRRSV-specific antibodies. Gross findings included pneumonia, absence of a detectable thymus, and small secondary lymphoid tissues. Histologically, lymph nodes, spleen, tonsils, and Peyer's patches were sparsely cellular with decreased to absent T and B lymphocytes.

2.A. Introduction

One hundred pigs from each of 2 Yorkshire lines divergently selected for feed efficiency (Cai et al. 2008) were enrolled, at 2–4 weeks of age, in a study of the genetic influence on response to Porcine Reproductive and Respiratory Syndrome virus (PRRSV) infection. This was

the 7th generation of partially inbred pigs. Pigs were arbitrarily distributed into pens of 16–18 pigs, with 1 week's acclimation before inoculation with PRRSV isolate NVSL97-7985. (Truong et al. 2004)

2.B. Materials and methods

T and B lymphocytes were identified by immunohistochemistry (IHC) using rabbit anti-human CD3 polyclonal antibody or mouse anti-human CD79a monoclonal antibody, respectively, followed by biotinylated goat anti-rabbit or anti- mouse immunoglobulin with avidin-HRPO and DAB chromagen (Ventana Medical), and counterstained with hematoxylin. Macrophages (histiocytes) were identified using lysozyme antibody. PRRSV and PCV2 IHC was performed on all the pigs. Prussian blue histochemial staining for detection of hemosiderin was performed on the lymph node of wild type and SCID pigs.

Viremia was quantified by standardized RT-PCR assays (Applied Biosystems, Foster City, California, or Tetracore, Rockville, Maryland). Results were reported as copies of RNA per PCR reaction volume. PRRSV-specific serum antibodies were detected using a standardized ELISA test (PRRS X3, IDEXX Laboratories, Westbrook, Maine). Results were reported as a sample/positive (S/P) ratio.

2.C. Results

Four pigs from the increased feed efficiency line developed poor body condition and illness and were euthanatized prematurely. The pigs were from 4 different litters, but pig Nos. 4, 6, and 124 had a common sire (Figure 2.1).

- Pig No. 4, a gilt, weaned at 16 days of age, was infected with PRRSV at 38 days and euthanatized at 54 days.
- Pig No. 6, a barrow, weaned at 27 days of age, was infected with PRRSV at 36 days and euthanatized at 47 days.
- Pig No. 109, a barrow, had been weaned at 21 days of age and was euthanatized at 34 before it was inoculated with PRRSV.
- Pig No. 124, a barrow, was weaned at 28 days of age and was euthanatized at 41 days of age before being inoculated with PRRSV.

At necropsy, all of the 4 pigs had rough hair coat and were smaller than littermates and other pigs enrolled in the study. All 4 pigs had decreased fat reserves and a body condition score (BCS) or 5/9. Postmortem examination of the 4 pigs was performed within 5 hours following death and carcasses had mild postmortem autolysis. The following gross findings were common to the 4 pigs: thymus was not visible, lymph nodes were small, and ileal Peyer's patches were inconspicuous (Figure 2.2). Spleen and tonsils were grossly normal, when compared to pen-mates. Bone marrow was not examined on any of the 4 pigs. Pig No. 4 had severe fibrinosuppurative bronchopneumonia, pig No. 6 had fibrinous synovitis in both tarsal joints, and pig No. 124 had dermatitis. *Streptococcus suis* was cultured from lung of pig No. 4.

Formalin fixed tissue sections from lung, heart, kidneys, stomach, liver, lymph nodes, spleen, tonsils, nasal turbinates, and intestines were submitted to the Kansas State Veterinary Diagnostic Laboratory for histopathology. The lymph nodes and spleen from the 4 pigs had abnormal architecture, characterized by globally decreased numbers of lymphocytes and near absence of lymphoid follicles with germinal centers in both tissue organs and absence of periarteriolar lymphoid sheaths in the spleen. The tonsils and Peyer's patches also had markedly reduced numbers of lymphocytes and absence of lymphoid follicles with germinal centers. Pigs

No. 6 and 109 had both interstitial pneumonia, and pig No. 109 had cytomegaloviral inclusions in epithelial cells of nasal submucosal glands and renal tubules.

Immunohistochemistry (IHC) for CD3 (T cell marker) and CD79a (B cell marker) revealed markedly decreased and nearly absent CD3-positive lymphocytes in lymph nodes and spleen, respectively. CD79a-positive lymphocytes were few in the lymph nodes and absent from the spleen (Figure 2.3). Histiocytic cells comprised the predominant cell population in lymphoid tissues and this was confirmed by staining with lysozyme antibody (Figure 2.5). Hemosiderin-laden macrophages were identified by positive reaction with Prussian blue histochemical staining in lymph node sections (Figure 2.4).

On day 0, all pigs were PRRSV negative by RT-PCR. By day 4 post inoculation (dpi), all pigs were PRRSV positive by RT-PCR, and they remained positive through day 11 post inoculation (Table 2.1). On day 4 after inoculation, all pigs were seronegative by ELISA. On day 11, pig Nos. 4 and 6 remained negative, whereas all other infected pigs had an antibody response to PRRSV. These data suggest that the affected piglets were incapable of initiating an antibody response after PRRSV inoculation.

2.D. Discussion

Although the PRRSV isolate used in this study normally results in seroconversion within 11 days post inoculation, the 2 pigs with severe lymphoid depletion that were inoculated with PRRSV failed to mount a measurable antibody response. All 4 pigs had a near absence of T and B lymphocytes in undersized secondary lymphoid tissues. No pathogens known to cause secondary immunodeficiencies were detected, and subsequent matings of the parents of the

affected pigs produced offspring with similar lesions. Collectively, these findings are consistent with an inherited primary immunodeficiency disorder.

Infection by porcine circovirus type 2 (PCV2) can result in lymphocyte depletion in lymphoid tissues. Co-infection with PCV2 and PRRSV can result in postweaning multisystemic wasting syndrome (Ladekjaer-Mikkelsen et al. 2002, and Nielsen et al. 2003) and affected animals are typically smaller than littermates due to progressive wasting. Although all inoculated pigs were positive for PRRSV by RT-PCR, PCV2 antigen was not detected by IHC in lymph node or lung sections from the 4 affected pigs, indicating that they did not have PCV-associated disease. Furthermore, there were no clinical signs or morphological lesions to suggest infection by any other pathogens known to cause lymphoid depletion in pigs, such as influenza virus, indicating that lymphoid hypoplasia was not a result of infection. Subsequent matings of the parents of these pigs have produced approximately 22% of piglets per litter with similar histologic lesions, suggesting that the affected pigs had a primary immunodeficiency. (Fischer et al. 1997)

2.E. References

1. Cai, W.D., Casey, D.S., and Dekkers, J.C.M. (2008). Selection response and genetic parameters for residual feed intake in Yorkshire swine. *J Anim Sci.* 86:287–298.

2. Fischer A, Cavazzana-Calvo M, de Saint Basile G, et al. (1997). Naturally occurring primary deficiencies of the immune system. *Annu Rev Immun.* 15:93–124.

3. Ladekjaer-Mikkelsen AS, Nielsen J, Stadejek T, et al. (2002) Experimental reproduction of postweaning multisystemic wasting syndrome (PMWS) in pigs experimentally infected with porcine circovirus type 2 (PCV2). *Vet Microbiol.* 89:97–114.

4. Nielsen J, Vincent IE, Botner A, et al. (2003) Association of lymphopenia with porcine circovirus type 2 induced postweaning multisystemic wasting syndrome (PMWS). *Vet Immunol Immunopathol*. 92:97–111.

5. Truong HM, Lu Z, Kutish GF, et al. (2004) A highly pathogenic porcine reproductive and respiratory syndrome virus generated from an infections cDNA clone retains the in vivo virulence and transmis- sibility properties of the parental virus. *Virology*. 325: 308–319.

Tables and Figures

Figure 2.1 Genealogic tree from the four initial pigs affected with SCID syndrome

The figure represents the line of descent of the four pigs in which the SCID syndrome was first recognized. Three of the pigs (Litter 1, 2, and 3, respectively) have a common male ancestor "Sire 1", whereas one of the pigs (Litter 4) derives from a different ancestor "Sire 2". Sire 1 and 2 both derive from a common ancestor. Sire 1 and 2 were subsequently mate to obtain litters of SCID pigs.

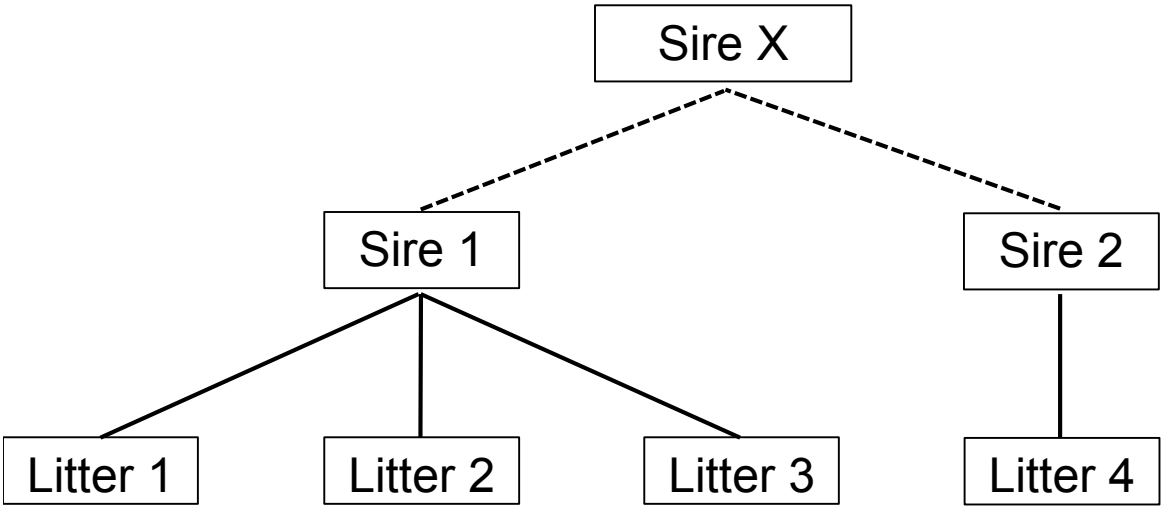

Figure 2.2 Gross findings on wild type and SCID piglets

Panel A shows the difference in size of the submandibular lymph nodes (dotted lines) between wild type and SCID pigs. Panel B shows the normal size and location of the thymus in a wild type pig and the absence in the SCID pig (yellow arrow heads). Panel C shows the presence of grossly visible Peyer's patches in the intestine of a wild type pig (black arrows), whereas in the SCID pigs they were not observable on gross examination.

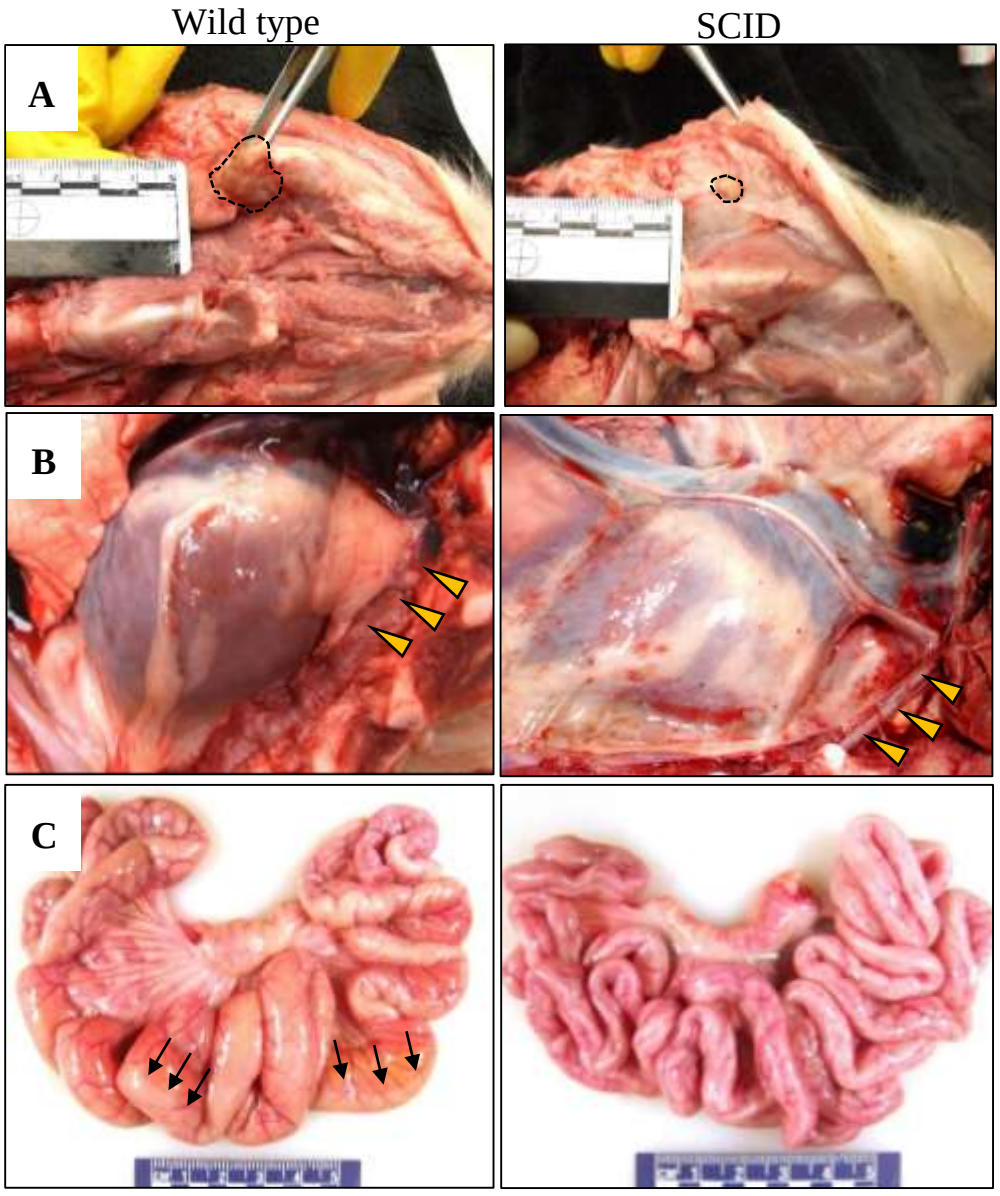

Figure 2.3 Histology of lymph node of wild type and SCID piglets

Representative histologic sections of lymph node from wild type (top row) and SCID piglets (bottom row) at approximately five weeks of age. The lymph node of the wild type pig is composed of lymphoid follicles with germinal centers (arrows), whereas in the SCID pig these structures are absent. A. H&E; 4X. B. Immunohistochemistry (IHC) for CD3 T cell marker, 4X. C. IHC for CD79a B cell marker, 4X.

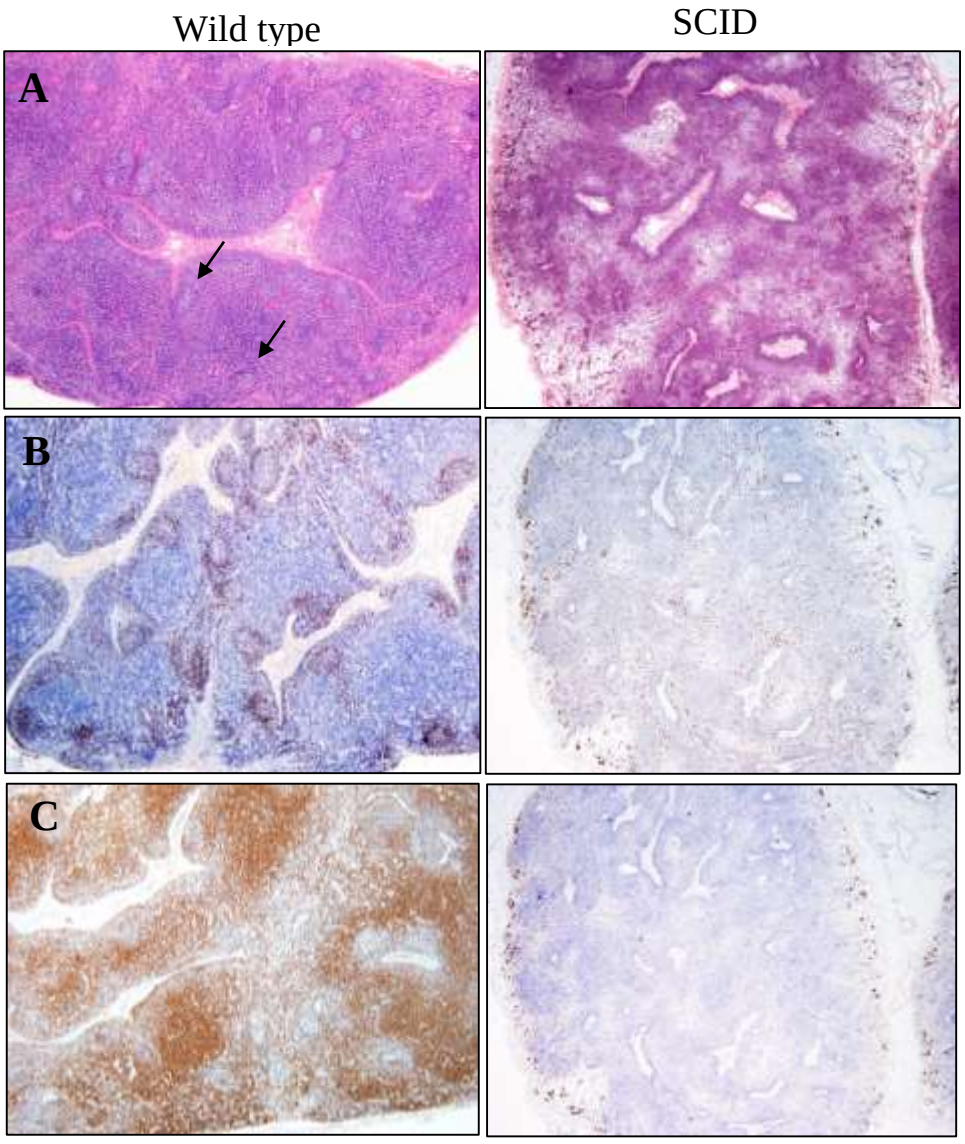

Figure 2.4 Pearl's Prussian blue staining of lymph node in SCID pig

Histochemical staining using Pearl's Prussian blue demonstrates the presence of hemosiderin pigment (which stains with blue) within the macrophages in the cortex of the lymph node of a SCID pig. (Counterstaining with brazilliant staining, magnification 2X).

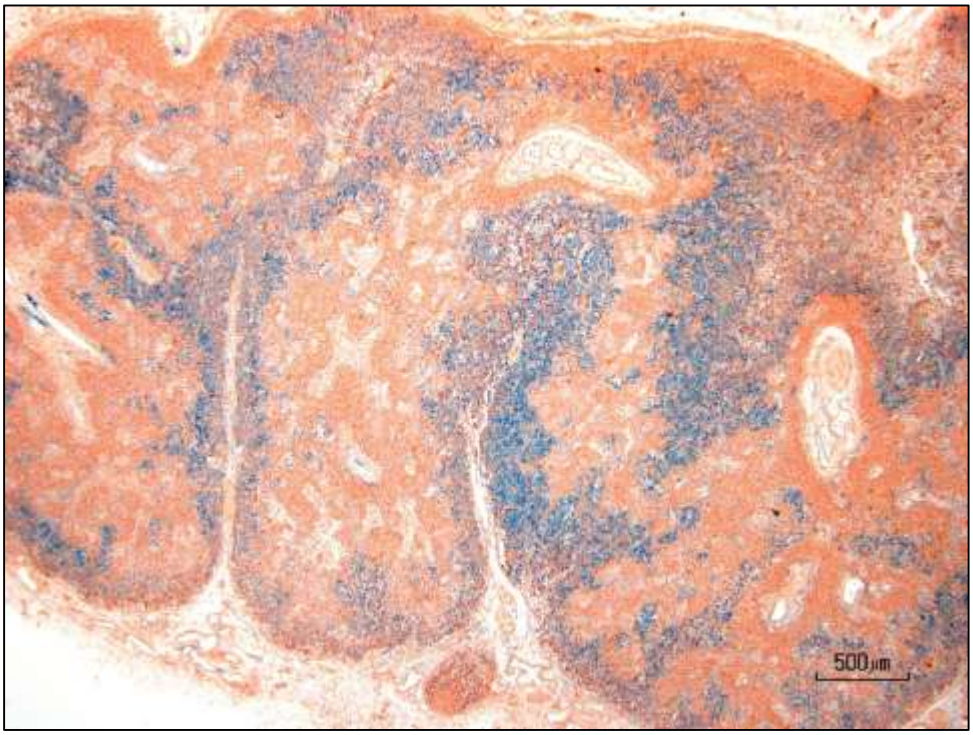

Figure 2.5 Lysozyme immunohistochemical staining of lymph node from a SCID pig

The image represents the lymph node of a SCID pig stained with antibodies for lysozyme (stained in brown), a marker of macrophages. The majority of the cells present on the lymph node are macrophages (brown) and stromal cells. Insert: The arrows point to lysozyme positive macrophages (dark brown) that also contain hemosiderin within their cytoplasm (golden granules). (Hematoxylin counterstain, magnification 10X).

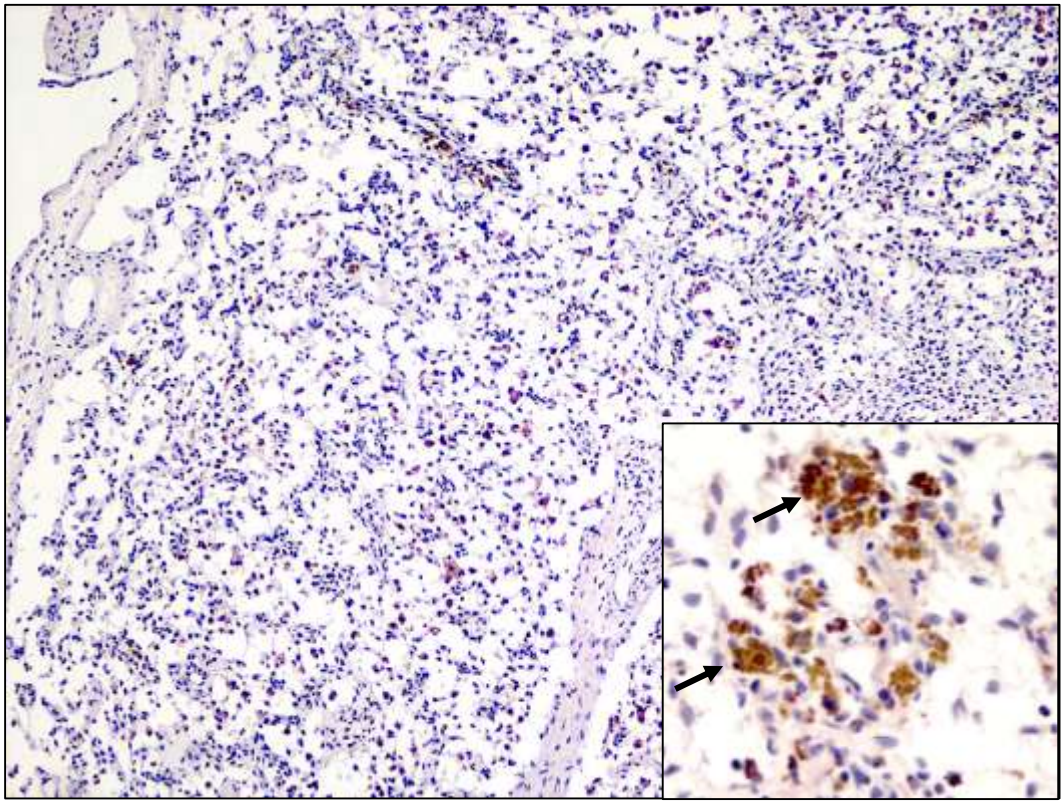

Table 2.1 ELISA and RT PCR results after infection with Porcine Reproductive and Respiratory Syndrome virus (PRRSV)

	Day 4		Day 7		Day 11	
Pig ID	ELISA[a]	PCR[b]	ELISA	PCR	ELISA	PCR
Pig 4	0.0	3.3	0.0	5.8	0.0	5.9
Pig 6	0.0	3.3	ND	3.8	0.0	6.7
Normal pigs[c]	0.0 (0)	5.4 (100)	0.25 (19)	6.2 (100)	2.0 (100)	6.0 (100)

Abbreviations: ND, not done

[a]ELISA results are reported as an S/P ratio. An S/P ratio greater than 0.39 is considered positive for PRRSV

[b]PCR results expressed as log10 quantity of viral RNA per reaction

[c]PCR results for normal pigs represent the mean of 8 pen mates. ELISA results are the mean for 190 pigs. The number in parenthesis is the percent pigs that were PCR positive or seropositive (S/P ratio > 0.39)

Chapter 3 - Naturally-occurring severe combined immunodeficiency (SCID) in pigs is due to defect in B and T cells

Catherine L. Ewen[1], Ada G. Cino-Ozuna[1], H He[1], M.A. Kerrigan[1], J.C.M. Dekkers[2], C.K. Tuggle[2], R.R.R. Rowland[1], C.R. Wyatt[1]

[1]Department of Diagnostic Medicine/Pathobiology, 1800 Denison Avenue, Manhattan, KS 66506, United States

[2]Department of Animal Science, Iowa State University, Ames, IA 50011, United States

Abstract

Severe combined immunodeficiency (SCID) is the result of a set of inherited genetic defects which render components of the immune response nonfunctional. In Arabian horses, Jack Russell terriers, and mice, the disorder is a consequence of the absence of T and B lymphocytes, while natural killer (NK) cell and other leukocyte populations remain intact. Preliminary analysis of a naturally acquired form of inherited SCID in a line of pigs showed several defects in the architecture and composition of secondary lymphoid organs. In this study, a quantitative assessment of lymphocyte populations in affected and normal littermates showed depleted T or B lymphocyte populations in affected pigs; however, NK cells and neutrophils were present in numbers comparable to unaffected littermates. The results indicate that the immune defect in pigs shares the same features as other SCID-affected species.

3.A. Introduction

Severe combined immunodeficiency (SCID) refers to a set of inherited disorders first described in children in the 1960s, and subsequently identified in a limited number of animal

species, including horses, mice, and dogs (Bauer *et al.,* 2009; Meek *et al*., 2001; Perryman, 2004). In humans and animals the disorder involves defects in both humoral and cellular immune functions. As an example, mutations in the catalytic subunit of DNA-dependent protein kinase (DNA-PKcs) are responsible for the SCID phenotype in C.B-17 mice, Arabian foals, and Jack Russell terriers, while X-linked mutations in the gene encoding the gamma chain of the IL-2 receptor are implicated in the defect in Bassett Hounds and Cardigan Welsh Corgis (Bauer *et al*., 2009; Bell *et al*., 2002; Blunt *et al*., 1995; Bosma and Carroll, 1991; Danska *et al*., 1996; Meek *et al*., 2001; Perryman, 2004). Affected animals are typically leukopenic with hypoplastic secondary lymphoid tissues. The thymus is absent, or markedly reduced in size and lacking in cortico-medullary delineation due to markedly reduced numbers of thymocytes. Lymph nodes contain few identifiable lymphocytes, but preserve the basic stromal structure and sinus pattern. Splenic lymphoid follicles and germinal centers are absent and are replaced by stromal cells, fibro-blasts, and macrophages (Bosma and Carroll, 1991; Custer *et al*., 1985; Bell *et al*., 2002; Lunn *et al.,* 1995; McGuire and Poppie, 1973; Meek *et al*., 2001). Even though there are few lymphocytes in SCID animals, monocytes, granulocytes, megakaryocytes, erythrocytes, and NK cell numbers remain normal (Bosma and Carroll, 1991; Custer *et al.*,1985; Lunn *et al.,* 1995).

We recently described a line of Yorkshire pigs that had been bred for increased feed efficiency, which produces offspring with an apparent SCID-like disorder (Cino-Ozuna *et al*., 2013). Phenotypic characteristics include lymphoid hypoplasia with the absence of germinal centers. Immunohistochemical staining of lymph nodes with polyclonal anti-CD3 (T cells) and anti-CD79α (B cells) antibodies reveals few positive cells. Additionally, affected piglets fail to produce antibodies in response to viral infection and are able to support the growth of human melanoma and pancreatic carcinoma cells (Basel *et al.,* 2012). Although the exact mutation

involved in the SCID phenotype has not been described, there is no sex predilection, since both barrows and gilts are affected at a similar frequency. While suckling, affected piglets appear normal and are indistinguishable from unaffected littermates, but soon after weaning begin to show clinical signs such as reduced growth, lethargy, the appearance of skin lesions, and respiratory distress, the result of overwhelming opportunistic infections. Survival past 60 days of age has not been observed.

The purpose of this study was to further elucidate the SCID phenotype by enumerating circulating white blood cell populations.

3. B. Materials and methods

Prior to initiating experiments involving animals, all work was approved by university biological safety and animal care and use committees. SCID pigs and unaffected normal littermates were derived from matings between immunocompetent heterozygous parents, from a line of commercial Yorkshire pigs that had been further bred for increased feed efficiency (Cino-Ozuna *et al.*, 2013). In total, the data collected were from 11 litters, comprising a total of 128 piglets, including 34 with SCID. Each experiment was designed based on the number of available heterozygous sows. The number of piglets available for each experiment and the number of SCID piglets in each litter was determined after the piglets were born.

For the SCID pigs, the immune suppressed phenotype became apparent within a few days to two weeks after weaning. Pigs became weak, grew at a slower rate (Figure 3.1), and exhibited a variety of clinical signs, the result of opportunistic infections (Cino-Ozuna *et al.*, 2013). Pigs eventually became moribund and were humanely euthanized.

All affected pigs were necropsied. Tissues were immediately fixed in 10% buffered formalin, embedded in paraffin, and sectioned at thickness of 5µm. Tissue sections were deparaffinized and stained with hematoxylin and eosin (H&E) using an automated procedure. Tissue processing, sectioning and staining were carried out as standard diagnostic procedures performed by the Kansas State Veterinary Diagnostic Laboratory. For the purpose of comparison, a representative number of unaffected normal healthy pigs were selected for necropsy.

Complete blood counts (CBCs) on heparinized blood were performed using an automated cell counter at the Iowa State Diagnostic Laboratory. The diagnostic labs were blind as to the nature of the samples. For white blood cells (WBC) and lymphocytes, the results were reported as WBC/µl and lymphocytes/ µl, respectively.

For antibody staining of lymphocyte populations, 100 µl aliquots of whole blood were placed in 12 mm × 75 mm polystyrene flow cytometry (FACS) tubes and incubated for10 min at room temperature in the presence of 10% normal mouse serum. Primary antibodies included fluorescein isothiocyanate (FITC)-conjugated mouse anti-porcine CD3ε (clone PPT3; Southern Biotech, Birmingham, AL, USA), allophycocyanin (APC)-conjugated mouse anti-porcine CD21 (clone BioBB6-11C9; BD Biosciences, San Jose, CA, USA) and R-phycoerythrin (R-PE)-conjugated mouse anti-porcine CD16 (clone G7; AbD Serotec, Raleigh, NC, USA. Table 3.1). Primary antibodies were diluted 1:20 in PBS, after which 50 µl was added to the whole blood and the mixtures incubated for 30 minutes at room temperature. Red blood cells were lysed by the addition of 1× multispecies lysis solution (eBioscience, San Diego, CA, USA). Cells were then washed twice in PBS with 2% BSA (Fraction V; Hyclone, Logan, UT, USA) and immediately analyzed on an EC800 flow cytometer (Sony Biotechnology, Champaign, IL, USA)

with FCS Express 4 software (De Novo Software, Glendale, CA, USA). A total of 100,000 leukocytes were collected for each sample. Absolute cell counts were calculated directly by EC800 software (version 1.3).

3.C. Results and discussion

Representative pictures of the lymphoid tissues from the pigs used in this study are shown in Figure 3.2. Follicles in the lymph nodes and spleen from normal pigs were composed of developing germinal centers rimmed by a mantle zone of lymphocytes; while, in the SCID pigs, follicles and germinal centers were absent. Peyer's patches from nor-mal littermates possessed well-defined and tightly packed lymphoid follicles with germinal centers, which markedly expanded the lamina propria mucosa and submucosa of the ileum. In contrast, Peyer's patches of SCID pigs were markedly reduced in size due to scarcity of lymphocytes, and the lymphoid follicles with germinal centers were absent. While the thymus of normal pigs contained well-defined medullary and cortical areas (Figure 3.2), the thymus of SCID pigs showed a substantial reduction in the number of lymphocytes and the absence of differentiation between the cortical and medullary regions. The microscopic changes observed in the lymphoid organs of SCID pigs, including results for immunohistochemical staining, are summarized in Cino-Ozuna *et al*. (2013) and share similarities to the changes reported earlier by one of us for the SCID horse (McGuire and Poppie, 1973; Wyatt *et al*., 1987).

The analysis of peripheral leukocyte populations began with the collection of complete blood counts (CBCs) from five litters of pigs derived from the mating of heterozygous parents. Plotting total WBC counts versus lymphocytes for 59 offspring showed that pigs could be divided into two distinct groups. The first group, identified by solid circles in Figure 3.3, was

located in the lower left corner of the graph. Based on histopathology of tissues, as described in Figure 3.2, all pigs in this group possessed the SCID phenotype; whereas representative pigs from the other group were normal. The mean number of WBC for the SCID group was 3.1 ± 0.9 cells/µl versus 6.9 ± 1.8 cells/µl for normal pigs. The difference between the two groups was significant, ($p < 0.0001$, Student's t-test). For lymphocytes, the means were 0.8 ± 0.4 and 4.0 ± 1 for SCID and normal pigs, respectively. The difference between the two groups was significant ($p < 0.0001$, Student's t-test). The analysis of CBC results shows that WBC and lymphocyte numbers in the blood are reduced. Therefore, relatively low numbers of WBC and lymphocytes can be used to rapidly identify pigs with the SCID phenotype. Furthermore, as illustrated in Figure 3.3, 14 of the 59 pigs (24%) were in the low lymphocyte (SCID) group, a percentage close to the Mendelian fraction of one quarter that would be predicted for the outcome from the mating of heterozygous parents.

A more detailed analysis of granulocyte and lymphocyte counts taken during the first 21 days after birth is presented in Figure 3.4. Mean neutrophil counts (Fig. 3.4A) were initially higher for both normal and SCID groups (days 4 and 9), and by day 13 were reduced. Statistical analysis showed that the differences in neutrophil counts between normal and SCID pigs were not significant. In contrast, total lymphocyte numbers (Fig. 3.4B) were significantly lower ($p < 0.05$) for pigs possessing the SCID phenotype compared to unaffected littermates. For the SCID pigs, numbers remained well below the 2.0 lymphocytes/l cutoff at each time-point. Together, these results showed reduced numbers of lymphocytes in pigs with the SCID phenotype and are consistent with the lymphocyte depletion seen in tissues. Additionally, the results also showed that the SCID defect did not extend to granulocytes.

The analysis of major subsets of peripheral blood lymphocytes was performed by determining the absolute numbers of $CD3^+$ (T cells), $CD21^+$ (B cells), and $CD16^+$ (NK cells) lymphocytes in whole blood. As illustrated in Figure 3.5, the analysis in whole blood was performed by drawing an inclusion gate around the lymphocyte population of cells. The configuration of the lymphocyte inclusion gate in SCID and normal blood was confirmed by staining with anti-CD3 to label T lymphocytes. Analyses were performed using only cells located within the lymphocyte gate. The results, shown in Figure 3.6, show that both CD3- and CD21-positive cells were nearly absent in the peripheral blood of SCID pigs. The differences between the unaffected and affected piglets were highly significant ($p < 0.0001$). The small numbers of CD3- and CD21-positive cells that were detected in the SCID group likely represented non-specific staining for the assay. The lymphocyte population was primarily composed of $CD16^+$ NK cells. The results were confirmed in subsequent experiments, using a secondary antibody with FITC conjugate (Figure 3.6). It should be noted that CD16 is expressed on several different cell types, including macrophages, blood-derived dendritic cells, and eosinophils, in addition to NK cells (Mair *et al.*, 2014). However, since NK cells possess the light scatter properties of lymphocytes, only the $CD16^+$ cells that fell within the lymphocyte gate were recorded as NK cells (Figure 3.7). Although the mean number of CD16-positive lymphocytes in this study was lower in the affected pigs, the difference was not statistically significant ($p = 0.5466$). The results show that the primary peripheral lymphocyte defect in SCID pigs is the depletion of B and T cells.

In SCID animals, such as dogs, mice, and horses, normal granulocyte and NK cell numbers are found in blood; whereas, B and T cells are markedly decreased or absent. It is the absence of B and T cells that explains the lack of acquired immune functions. The quantitative

analysis of SCID pig tissues stained with anti-CD3 and anti-CD21 showed an almost complete absence of B and T cells in the periphery. The absence of peripheral B and T cells supports the histological observations for primary and secondary lymphoid organs, including small size and the absence of follicles and germinal centers (Cino-Ozuna *et al*., 2013). In contrast, affected pigs appear to have normal numbers of NK cells and granulocytes. However, the inability of SCID piglets to reject human xenografts, as previously reported in Basel *et al*. (2012), suggests that NK cells are functionally impaired. The absence of NK cell function in the presence of normal NK cell numbers is observed in the SCID horse. Depressed NK function is a consequence of the absence of T cell-produced IL-2 (Magnuson *et al.,* 1987). A lack of T cell cytokines may explain the apparent loss of normal NK function in the SCID pig. Thus, these SCID pigs possess a T- and B-lymphocyte negative, NK cell-positive phenotype, features consistent with the phenotypic properties of SCID in other animal species. Additional studies are in progress to further characterize the CD16-positive lymphocytes.

Recently, a SCID pig has been developed from the manipulation of the RAG2 gene (Lee *et al*., 2014). These pigs were shown to support early development of human stem cells, and to tolerate engraftment of allogeneic pig stem cells. The model is of interest in transplantation research. The SCID phenotype described here and by Cino-Ozuna *et al*. (2013) and Basel *et al*. (2012), was discovered as a result of a breeding program to enhance an unrelated trait. Therefore, it is of interest to understand the properties of the SCID mutation and its potential impact on production pig populations.

3.D. References

18. Basel, M.T., Balivada, S., Beck, A.P., Kerrigan, M.A., Pyle, M.M., Wyatt, C.R., Rowland, R.R.R., Anderson, D.E., Troyer, D.L. (2012). Human xenografts are not rejected in a naturally occurring immunodeficient porcine line: a human tumor model in pigs. *Biores. Open Access* 1, 63–68.

19. Bauer, T.R., Adler, R.L., Hickstein, D.D. (2009). Potential large animal models for gene therapy of human genetic diseases of immune and blood cell systems. *ILAR J.* 50, 168–186.

20. Bell, T.G., Butler, K.L., Sill, H.B., Stickle, J.E., Ramos-Vara, J.A., Dark, M.S. (2002). Autosomal recessive severe combined immunodeficiency of Jack Russell Terriers. *J. Vet. Diagn. Invest.* 14, 194–204.

21. Blunt, T., Finnie, N.J., Taccioli, G.E., Smith, G.C.M., Demengeot, J., Gottlieb,J.M., Mizuta, R., Varghese, A.J., Alt, F.W., Jeggo, P.A., Jackson, S.P., 1995.Defective DNA-dependent protein kinase activity is linked to V(D)J recombination and DNA repair defects associated with the murine scid mutation. *Cell* 80, 813–823.

22. Bosma, M.J., Carroll, A.M. (1991). The SCID mouse mutant: definition, characterization and potential uses. *Ann. Rev. Immunol.* 9, 323–330.

23. Cino-Ozuna, A.G., Rowland, R.R.R., Nietfeld, J.C., Kerrigan, M.A., Dekkers,J.C., Wyatt, C.R. (2013). Preliminary findings of a previously unrecognized porcine primary immunodeficiency disorder. *Vet. Pathol.* 50,144–146.

24. Custer, R.P., Bosma, G.C., Bosma, M.J. (1985). Severe combined immunodeficiency (SCID) in the mouse. Pathology, reconstitution, neoplasms. *Am. J. Pathol.* 12, 464–477.

25. Danska, J.S., Holland, D.P., Mariathasan, S., Williams, K.M., Guidos, C.J. (1996). Biochemical and genetic defects in the DNA-dependent protein kinase in murine scid lymphocytes. *Mol. Cell. Biol.* 16, 5507–5517.

26. Lee, K., Kwon, D.-N., Ezashi, T., Choi, Y.-J., Park, C., Ericsson, A.C., Brown,A.N., Samuel, M.S., Park, K.-W., Walters, E.M., Kim, D.Y., Kim, J.-H., Franklin, C.L., Murphy, C.N., Roberts, R.M., Prather, R.S., Kim, J.-H. (2014). Engraftment of human iPS cells and allogeneic porcine cells into pigs with inactivated RAG2 and accompanying severe combined immunodeficiency. *Proc. Natl. Acad. Sci. U. S. A.* 111, 7260–7265.

27. Lunn, D.P., McClure, J.T., Schobert, C.S., Holmes, M.A. (1995). Abnormal pat-terns of equine leukocyte differentiation antigen expression in severe combined immunodeficiency foals suggests the phenotype of normal equine natural killer cells. *Immunology* 84, 495–499.

28. Magnuson, N.S., Perryman, L.E., Wyatt, C.R., Mason, P.M., Talmadge, J.E. (1987). Large granular lymphocytes from SCID horses develop potent cytotoxic activity after treatment with human recombinant Interleukin 2. *J. Immunol.* 139, 61–67.

29. Mair, K.H., Sedlak, C., Kaser, T., Pasternak, A., Levast, B., Gerner, W., Saalmuller, A., Summerfield, A., Gerdts, V., Wilson, H.L., Meurens, F. (2014). The porcine innate immune system: an update. *Dev. Comp. Immunol*.45, 3321–3343.

30. McGuire, T.C., Poppie, M.J. (1973). Hypogammaglobulinemia and thymichypoplasia in horses: a primary combined immunodeficiency disorder. *Inf. Immun.* 8, 272–277.

31. Meek, K., Kienker, L., Dallas, C., Wang, W., Dark, M.J., Venta, P.J., Huie, M.L.,Hirschhorn, R., Bell, T. (2001). SCID in Jack Russell Terriers: a new animal model of DNA-PKcs deficiency. *J. Immunol.* 167, 142–2150.

32. Perryman, L.E. (2004). Molecular pathology of severe combined immunodeficiency in mice, horses, and dogs. *Vet. Pathol.* 41,95–100.

33. Wyatt, C.R., Magnuson, N.S., Perryman, L.E. (1987). Defective thymocyte maturation in horses with Severe Combined Immunodeficiency. *J. Immunol.* 139, 4072–4076.

Tables and Figures

Figure 3.1 Clinical appearance of wild type and SCID pig after weaning

The image shows a SCID piglet (arrow) and a wild type piglet from the same litter. SCID pigs have smaller size and a rougher hair coat than wild type litter mates (right) after weaning.

Figure 3.2 Histology of wild type and SCID littermates.

Representative microhistology of primary and secondary lymphoid tissues from normal and SCID piglets. This example shows tissues from normaland SCID pigs at 3 approximately three weeks of age. Thin sections were stained with hematoxylin and eosin (H&E). The magnification for spleen and thymus was 2X. The magnification for lymph node and intestine was 4X.

Key: GC, germinal center inside a follicle; F, area with follicles; M, medulla; C, cortex

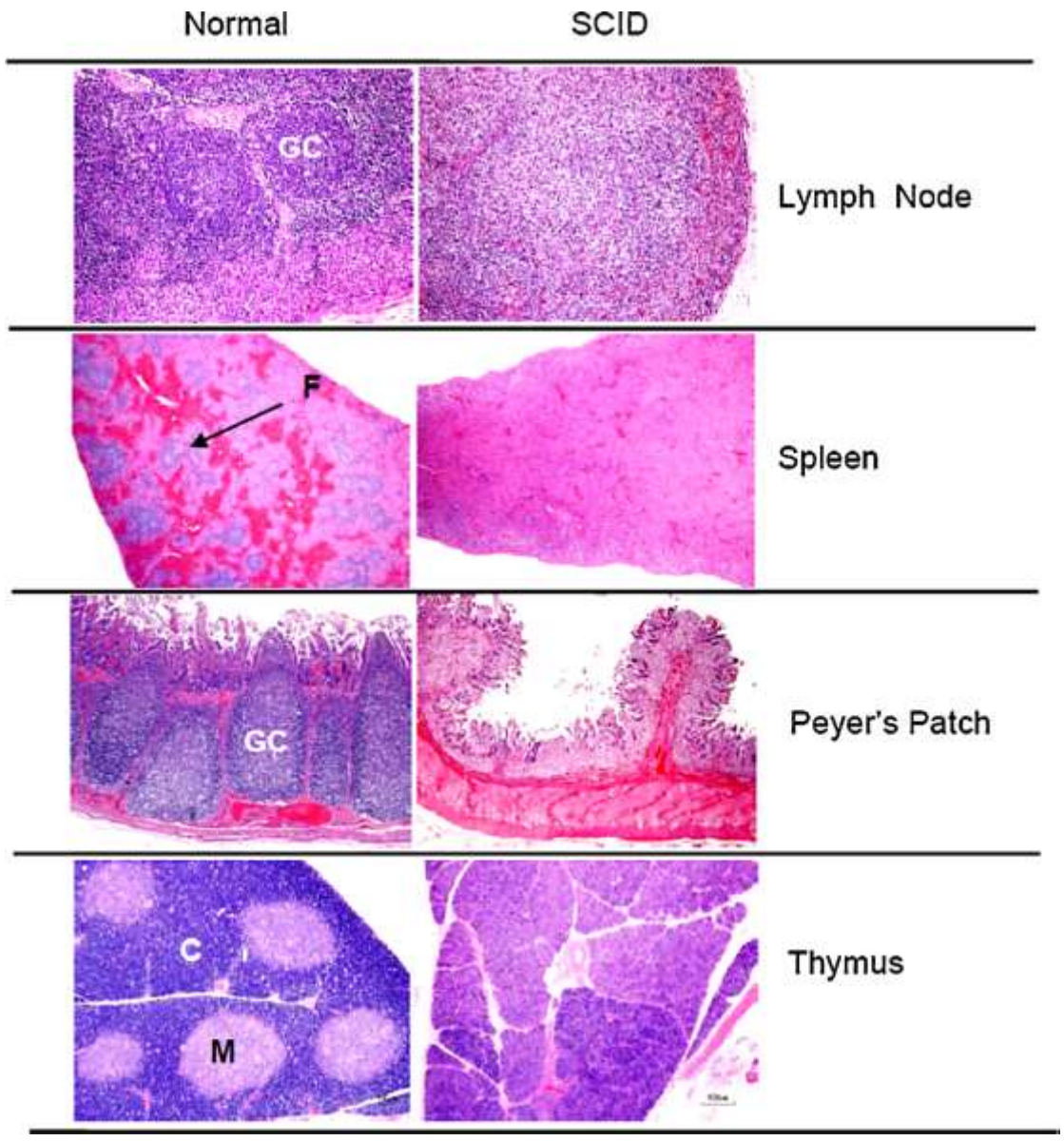

Figure 3.3 Total white blood cell versus lymphocyte counts in normal and affected piglets.

CBC measurements of 59 piglets 8–22 days of age werecollected from five litters derived from heterozygous parents. The closedcircles represent 14 affected pigs that showed the characteristic SCID-associated histopathology described in Fig. 1. The open circles are from normal littermates.

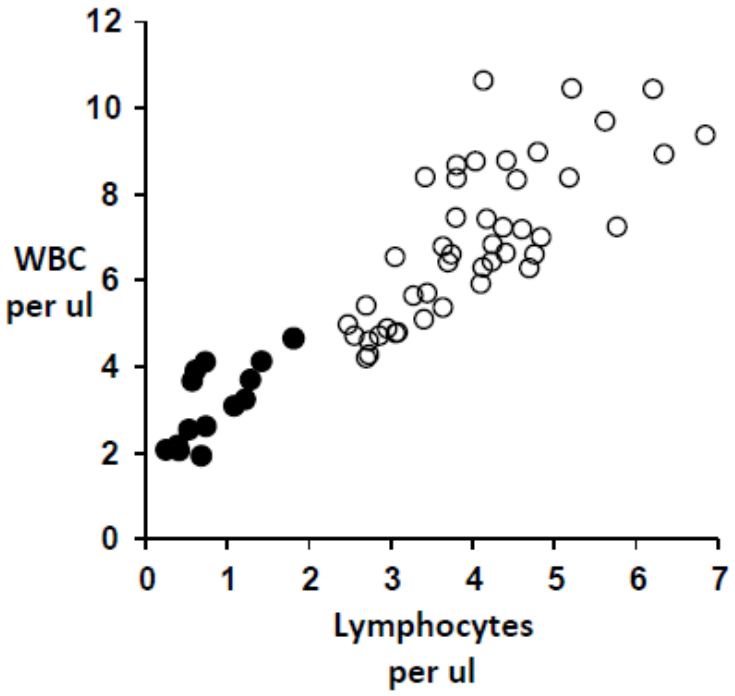

Figure 3.4 Mean neutrophil and lymphocyte numbers over the first 22 days after birth for SCID and normal pigs.

The upper and lower figures show theresults for numbers of neutrophils and lymphocytes in peripheral blood, respectively. The data are from two litters of pigs derived from the mating of heterozygous parents. The open circles are the normal littermates and the closed circles the SCID pigs. Horizontal bars show mean and standard deviation. At the end of the study the SCID and normal phenotypes were confirmed by histology of lymphoid organs. Statistical comparisons between normal and SCID groups for each day were made using Student's t-test.
Key: ns, not significant ($p > 0.05$); C, control pigs; S, SCID pigs.

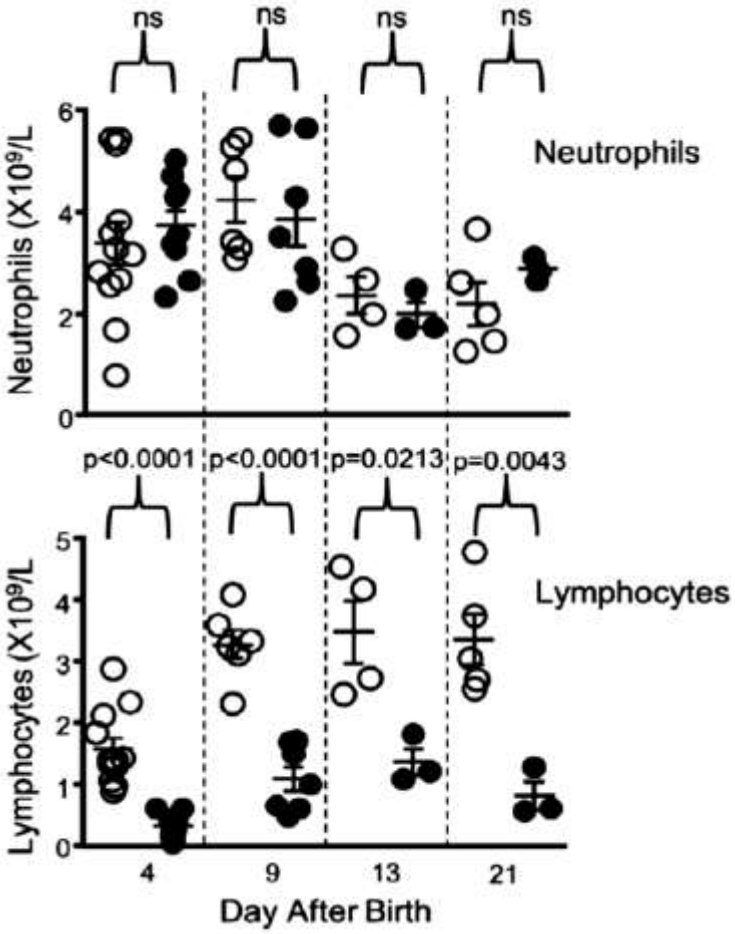

Figure 3.5 Flow cytometric analysis of blood from wild type and SCID pigs

Total white blood cell versus lymphocyte counts in normal and affected piglets. CBC measurements of 59 piglets 8–22 days of age were collected from five litters derived from heterozygous parents. The closed circles represent 14 affected pigs that showed the characteristic SCID-associated histopathology described in Fig. 1. The open circles are from normal littermates. Gating on lymphocytes in whole blood. The upper panels show the light scatter properties of the major white blood cell populations in whole blood after lysis of red cells. The populations of granulocytes, monocytes and lymphocytes are labeled in the figure. The lower panels show that all CD3+cells fall within the lymphocyte gate.

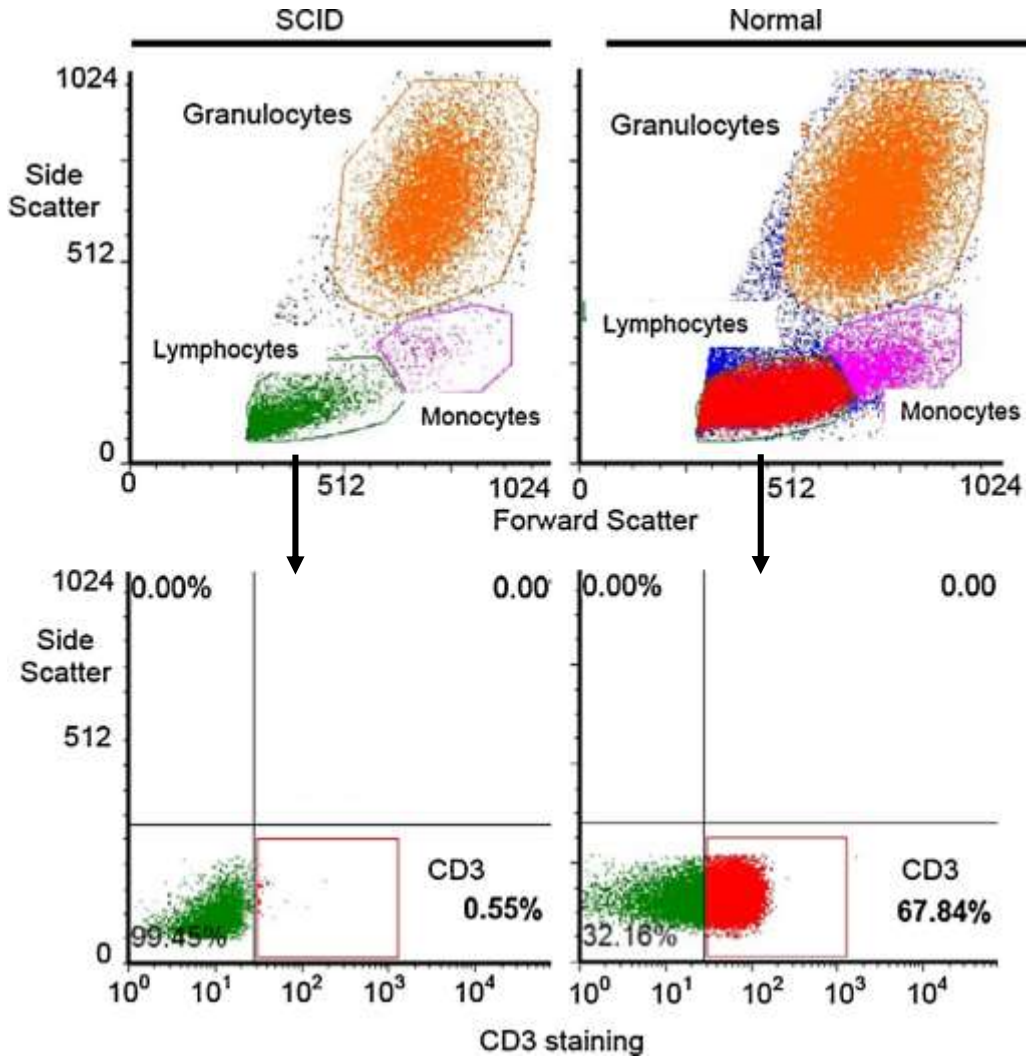

Figure 3.6 Total number of natural killer (NK) cells in wild type and SCID piglets on a follow-up study.

The plots show detection by flow cytometry of CD16 (NK cells), using a FITC-conjugated secondary detecting antibody on a follow up study. $CD16^{+}$ lymphocytes are located on the bottom-right quadrant of the plot. The plots were gated on lymphocytes. Quadrants were established using an isotype control.

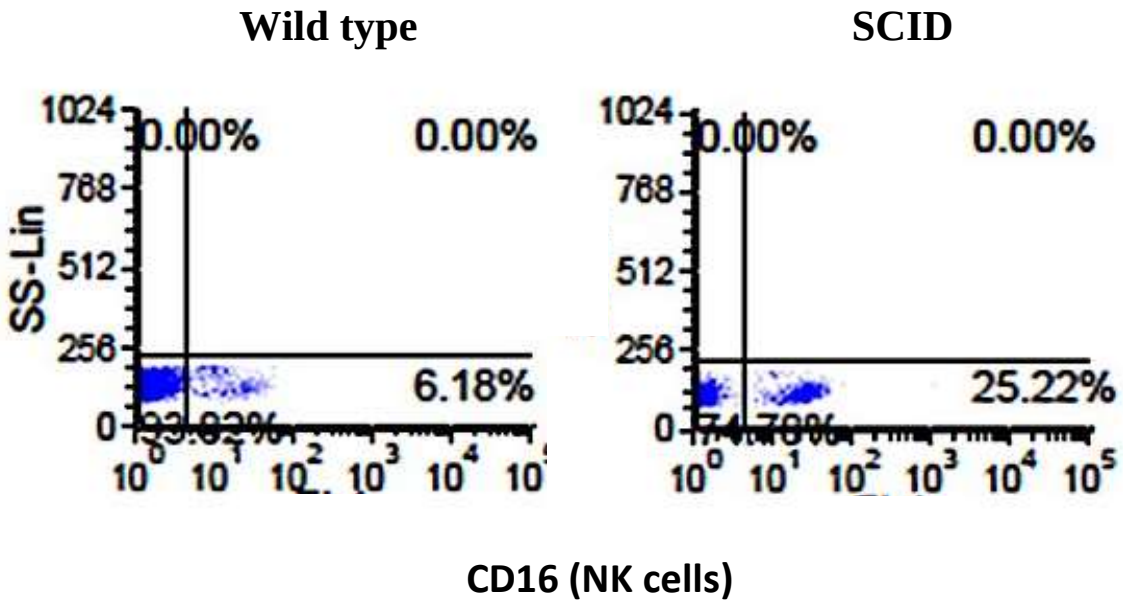

Figure 3.7 Total comparison of subsets of lymphocytes in the blood of wild type and SCID pigs.

Major lymphocyte subpopulations in the peripheral blood of normal and SCID littermates. The data are from a single litter derived from a single heterozygous mating. The figure shows the mean and standard deviation for five normal and three SCID pigs, obtained at approximately one week after birth. Asterisk identifies statistically significant differences between normal and SCID groups, $p < 0.0001$ (Student's t-test).

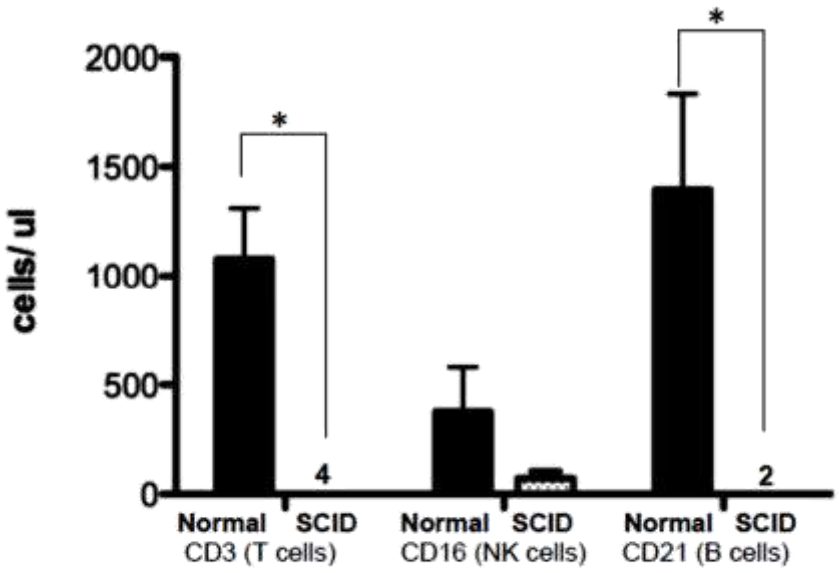

Table 3.1 Antibodies used for flow cytometry.

Primary antibody	Fluorochrome	Clone
CD3ε	Fluorescein isothiocyanate (FITC)	PPT3
CD21	Allophycocyanin (APC)	BioBB6-11C9
CD16	R-phycoerythrin (R-PE)	G7

Chapter 4 - Pigs with severe combined immunodeficiency (SCID) fail to develop pulmonary disease after infection with Porcine Reproductive and Respiratory Syndrome Virus (PRRSV)

Abstract

Infection of alveolar macrophages with porcine reproductive and respiratory syndrome virus (PRRSV) is followed by interstitial pneumonia with the infiltration of lymphocytes and macrophages. However, the mechanisms leading to interstitial pneumonia are largely unknown. In this study, seven pigs with a genetic severe combined immunodeficiency (SCID) along with two normal littermates were infected with PRRSV at 21-days of age. At 10 days after infection, lesions in the lungs of wild type pigs showed signs indicative of acute PRRS, including interstitial pneumonia, perivascular edema, and increased $CD3^+$ (T cell) staining surrounding pulmonary blood vessels. PRRS-associated lesions were absent in the infected SCID littermates; however, four SCID pigs showed signs of pneumonia, the likely result of a secondary bacterial infection. Phenotypic analysis showed similar expression of CD172, SLA-II, and CD163 expression on wild-type and SCID macrophages. PRRSV PCR showed the presence of virus in alveolar macrophages, bronchial alveolar lavage fluid (BALF) and serum. The results demonstrate that the productive infection of macrophages is not the principal source for the pulmonary pathology observed during acute PRRSV infection.

4.A. Introduction

Regardless of the route of infection, acute infection with porcine reproductive and respiratory syndrome virus (PRRSV) is characterized by interstitial pneumonia and the recruitment of lymphocytes to the lung (Costers, *et al.,* Archives of Virology, 2008). PRRSV interstitial pneumonia can vary from mild to severe lymphocytic and histiocytic interstitial pneumonia with septal thickening and type 2 pneumocyte hyperplasia and hypertrophy, the latter most commonly appearing in severely affected lungs. (Halbur *et al*., Vet Path, 1995 and 1997; Rossow KD, Vet Path, 1998). The more severe forms of respiratory disease are linked to infection with co-pathogens, such as porcine circovirus type 2 (PCV2) swine influenza virus (SIV), *Mycoplasma sp, Streptococcus suis, and Pasteurella multocida.* (reviewed in Opriessnig et al., 2011).

The activation of lung macrophages by viral infection leads to a rapid induction of adaptive immunity in the lung. Kim *et al*. (2008) and Hartwig *et al*. (2014) described the important role of alveolar macrophages for controlling replication, but are also involved in acute lung pathology. Presumably T cells are recruited to the lung and destroy infected cells, but at the same time stimulate the release of inflammatory cytokines or their cytotoxic activity, as demonstrated by Taylor *et al*. (1985). However, the role of alveolar macrophages or T cells in lung immunopathology after infection with PRRSV is largely unknown. One possible mechanism for clinical pathology is the direct destruction of alveolar macrophages (Thanawongnuwech *et al*., 1997). Alternatively, pathology may be the product of the T cell-stimulated release of pro-inflammatory cytokines.

The purpose of this study was to determine the role of T cells in lung pathology by incorporating the infection of pigs with severe combined immunodeficiency (SCID), which lack

functional T cells. SCID is a syndrome characterized by impaired adaptive immune responses and naturally occurs in humans, mice, horses, and dogs. In all four cases, the SCID phenotype is the result of the depletion of functional B and T cells. Recently, a naturally occurring SCID syndrome was reported by us for pigs (Cino-Ozuna *et al*., 2013), which originated from a line of partially inbred Yorkshire pigs undergoing breeding selection for increased feed efficiency. The SCID phenotype is the result of a recessive mutation that produces a marked lymphopenia and leukopenia, gross and microscopic lymphoid hypoplasia with the near absence of $CD3^+$ T cells and $CD79a^+$ B cells (Cino-Ozuna *et al*., 2013; Ewen *et al*. 2014). The paucity of lymphocytes translates into the absence of antibody responses to viral infection and the failure of pigs to reject human cancer cells (Basel *et al*., 2012). In a previous study, the course of PRRSV infection was followed in wild-type (WT) and SCID littermates (Chen *et al*. 2014). The results showed that viremia was significantly reduced in SCID pigs; however, by day 21, the trend was reversed, with higher viremia in the WT group.

4.B. Materials and methods

All experiments involving animals and viruses were performed in accordance with the Federation of Animal Science Societies (FASS) Guide for the Care and Use of Agricultural Animals in Research and Teaching and the USDA Animal Welfare Act and Animal Welfare Regulations, and approved by the Kansas State University institutional animal care and biosafety committees. Pigs were obtained from the cross of an immunocompetent heterozygous SCID +/- dam with a homozygous recessive SCID boar that was reconstituted with bone marrow cells from a WT littermate. The mating produced a total of nine pigs; three female and six male pigs.

Immunophenotyping for detection of SCID in pigs

The outline of the study is summarized in Figure 4.1. The presence of the SCID phenotype in each piglet was determined by flow cytometry on whole blood taken at two days after birth (Ewen *et al*, 2014). Primary antibodies used for surface staining of T cells, B cells, and NK cells markers included: R-phycoerythrin (RPE)-conjugate mouse anti-pig CD3ε (clone BB23-8E6, SouthernBiotech, Birmingham, AL, USA), allophycocyanin (APC)-conjugate mouse anti-pig CD21 (clone B-ly4, BD Pharmingen™, San Jose, CA, USA), and fluorescein isothiocyanate (FITC)-conjugate mouse anti-pig CD16 (clone G7, AbD Serotec, Raleigh, NC, USA). These antibodies were initially diluted 1:20 in PBS and 50 µl of the diluted antibody was added to 100 µl of whole blood. The solution was then incubated for 30 min in the dark at room temperature, to allow the attachment of the labelled antibodies to the respective cell surface targets. Following incubation, red blood cells were lysed using RBC Lysis Buffer™ (eBioscience, Inc. San Diego, CA USA). The remaining PBMCs were washed and resuspended in 200 µL PBS. A total of 100,000 white blood cells were collected and analyzed on EC800 flow cytometer (Sony Biotechnology, Champaign, IL, USA) using FCS Express 4 software (De Novo Software, Glendale, CA, USA).

PRRSV and mode of infection

At the time of weaning, or three weeks after birth, all piglets were infected with a Type II PRRSV isolate, P129-GFP (GenBank# AF494042). Pigs were infected with approximately 10^5 $TCID_{50}$ of virus in 2 ml of medium. The dose was split in half into two 1 mL syringes, one half delivered into the nares and the remaining injected intramuscularly in the caudal thigh. Piglets were housed in biosafety level (BSL)-2 facilities at the Large Animal Research Center (LARC)

at Kansas State University and monitored daily for clinical signs, until the study was finalized at 10 days after PRRSV infection.

Histopathology and immunohistochemistry

Lung, along with other tissues were immediately fixed in 10% buffered formalin, processed for sectioning, and stained with hematoxylin and eosin (H&E). Immunohistochemistry (IHC) staining for T cells was performed using an automated IHC staining procedure performed by the Kansas State Veterinary Diagnostic Laboratory. Briefly, T cells were stained with mouse anti-human CD3 monoclonal antibody (clone LN10, Leica Biosystems, Buffalo Groove, IL, USA). This antibody targets specifically the non-glycosylated surface epsilon chain of the CD3 molecule. Methylene bridges are formed during formalin fixation of the tissue sample, causing crosslinking of proteins and masking epitopes, preventing antibody binding. These bridges were treated with heat (heat-induced epitope retrieval) to allow the "unmasking" of the antigen epitopes, allowing the binding of antibodies to the target. Bound antibody was detected with biotinylated goat anti-mouse immunoglobulin, followed by DAB chromogen (Leica Biosystems, Buffalo Groove, IL, USA). Slides were counterstained with hematoxylin.

PCR on serum, BALF, and PAMs

PAMs were recovered from bronchoalveolar lavage fluid (BALF) and the technique was performed as described before (van Leengoed and Kamp, 1989), with some modifications. BALF was obtained by pouring 150 ml of ice-cold PBS into the pulmonary airway. After a

gentle massage, 100 ml of BALF were harvested and filtered through a 100 µm cell strainer (Midsci, St. Louis, MS, USA) to remove debris. The cell fraction containing the PAM cell population was recovered by centrifugation at 800 x *g* (1500 rpm) for 10 minutes and 4ºC. The pellet containing the PAMs was suspended at a concentration of 1 x 10^7 cells/mL in ice cold PBS and the cell suspension was kept at 4º C to avoid attachment of PAMs to the tube wall. PRRSV nucleic acid was detected by RT-PCR using an EZ-PRRSV™ MPX 4.0 Real Time RT-PCR Target-Specific Reagents (Tetracore®, Rockville, MD, USA). The assay was performed according to the manufacturer's instructions, and using a CFX96 Touch™ Real-Time PCR Detection System (Bio-Rad, Hercules, CA, USA). 50 µl of serum and BALF and a total of ~5 x 10^5 PAMs in 50 µl suspension were utilized for the PCR reactions.

Flow cytometry of PAMs

The phenotypic properties of WT and SCID porcine alveolar macrophages (PAMs) were assessed by staining PAMs with monoclonal antibodies against CD172, CD163, and MHC class II (SLA II, Table 4.2). The pellet recovered from the lung lavage was suspended in ice cold PBS at a cell concentration of 1 x 10^7 cells / ml. A 50 µl aliquot containing 5 x 10^5 PAMs was used for surface antibody staining with the following primary antibodies: RPE mouse anti-pig CD163 (clone 2A10/11, Serotec, Raleigh, NC, USA), mouse anti-pig CD172a (clone 74-22-15A, IgG2b, Washington State University, WA, USA), and mouse anti-pig MHC class II (SLA-II, clone MSA3, IgG2a, Washington State University, WA, USA). Primary antibodies were diluted at a ratio of 1:100-200 in ice cold PBS and 50 µl of the solution was added to the PAMs cell suspension. The mixture was incubated at 4º C and in the dark for 30 min. Primary antibodies for CD172 and MHC class II were not labeled with fluorochromes; therefore, secondary detection

antibodies targeting the specific immunoglobulin (Ig) subclasses used for the primary antibodies were added to the cell suspension. Secondary antibodies included: R-phycoerythrin-Cyanine 7 (PE/Cy®7)-conjugate goat anti-mouse IgG2b (Southern Biotech, Birmingham, AL, USA) that targeted CD172a and Peridinin-chlorophyll proteins/Cyanine 5.5 (PerCP/Cy®5.5)-conjugate rat anti-mouse IgG2a (BioLegend, San Diego, CA, USA) that targeted MHC class II. These antibodies were incubated at 4° C and in the dark for 30 minutes. Flow cytometry and data analysis were performed as described for lymphocytes before.

4.C. Results and discussion

The design of the current study was to compare lung pathology in wild type and SCID pigs at 10 days after infection with PRRSV, during the peak of PRRSV viremia.

Immunophenotyping of WT and SCID pigs

Based on forward and side scatter properties, the white blood cells were placed into granulocyte and mononuclear cell compartments (Figure 4.2). For the WT pigs, the $CD3^+$ cells were located within the compartment of cells possessing low forward and side scatter properties, confirming the location of lymphocytes. A representative plot from a SCID pig is shown for the purpose of comparison. As expected, the SCID pigs showed decreased numbers of cells with low forward and side scatter properties and only a few of these cells were $CD3^+$ cells. The remaining $CD3^-$ cells with low side and forward scatter properties were monocytes and NK cells (Ewen *et al.* 2014).

The surface phenotypic properties for the nine pigs used in this study are summarized in Table 4.3. The results showed that two pigs possessed relatively high numbers of $CD3^+$ T cells and $CD21^+$ B cells with mean concentrations of 778 cells/µl and 183 cells/µl, respectively. Both pigs were placed in the WT group. In sharp contrast, mean concentrations of $CD3^+$ T cells and $CD21^+$ B cells for the remaining seven pigs were 17±15 cells/µl and 0±0 cells/µl, respectively. These results are consistent with pigs possessing the SCID phenotype (Ewen et al., 2014). The concentration of $CD16^+$ lymphocytes, or NK cells, were similar for both groups (mean = 84 for WT pigs and 150+/-134 for the SCID group).

Clinical signs and necropsy findings

Pigs showed no clinical signs until 7-days after infection, when one WT pig (pig #6) and 3 SCID pigs (pigs #3, 8 and 9) developed eye infections, which were unrelated to PRRSV infection. In addition, SCID pig #3 developed an abscess on the intermandibular region. At 8- and 9-days post infection, the two WT pigs and two SCID pigs (#3 and #9) developed mild dyspnea, with one of the SCID pigs possessing a sporadic non-productive cough. The remaining SCID pigs were clinically normal. By 10-days post infection, the two WT pigs and SCID pigs #3 and #9 had moderately increased respiratory rates and exhibited open-mouthed breathing (Figure 4.3. Video). In addition, SCID pig #9 developed multiple cutaneous abscesses over the right forelimb along with a moderate fever.

On day 10, the pigs were euthanized in accordance with the AVMA Guidelines on Euthanasia. The euthanasia solution, sodium pentobarbital, 390 mg/ml was delivered at a dose of 1 ml per 10 lbs of body weight. A complete post-mortem examination was performed on all piglets. Upon gross examination, the lungs of the two WT pigs #1 and #6 showed evidence of

pneumonia (Figure 4.4.). The lungs were diffusely congested, had a firm texture, and the interlobular septae were moderately distended by edema fluid. The thoracic cavity contained approximately 15 and 25 ml of serous fluid, respectively. The results are consistent with the gross lung pathology observed during acute PRRSV infection. The lungs of two SCID pigs (#3 and #9) also showed lung pathology. The lungs appeared diffusely congested, firm, and had multifocal variably sized areas of hemorrhage. In addition, the pleural surface of pig #9 was covered by fine strands of fibrin. The remaining SCID pigs showed no evidence of pathology.

SCID pigs showed no evidence of PRRSV-associated pneumonia

The microscopic examination of the two WT pigs revealed moderate interstitial pneumonia characterized by interlobular and interalveolar septal thickening accompanied by the infiltration of mainly lymphocytes and macrophages (Figure 4.5.B). The alveolar spaces contained moderately increased numbers of macrophages. There was moderate perivascular edema and moderate to severe lymphocytic perivascular cuffing. Compared to a normal, age-matched PRRSV-negative pig (Figure 4.5.A), the anti-CD3 staining revealed accumulation of small numbers of T cells in the perivascular region of small to medium blood vessels. No $CD3^+$ T cells were observed in the lungs of the SCID pigs. Overall, the results for the two WT pigs are consistent with histological changes present during acute PRRSV infection (Halbur et al, 1995[a and b]). Two of the SCID pigs also exhibited a moderate pneumonia; however, the pneumonia was mainly the result of the accumulation of neutrophils along with alveolar macrophages (see Figure 4.5.D), which is not characteristic of PRRSV infection. Gram-positive bacteria were also present (Figure 4.6). These results are consistent with a primary bacterial pneumonia. The

remaining SCID pigs showed no evidence of pneumonia and the lungs were microscopically similar to an age-matched non-infected normal pig (compare Figure 4.5 panels A and C).

SCID and WT pigs were productively infected with PRRSV

One possibility for the absence of lung pathology in the SCID pigs was the lack of infection of alveolar macrophages with PRRSV. To determine if there was productive infection of PAMs in SCID pigs, PRRSV nucleic acid was measured in serum, PAMs, and bronchoalveolar lavage fluid (BALF) of WT and SCID pigs. The results for serum, BALF and PAMs are presented in Figure 4.7. The mean value in serum for all pigs was 5.0 log10 templates per ml, demonstrating that all pigs were productively infected. Furthermore, there were no significant differences in the viremia between WT and SCID pigs (Figure 4.8). PCR also detected virus nucleic acid in alveolar lavage cells. One SCID pig within the subgroup that showed no pulmonary pathology contained no detectable PRRSV, while the remaining no-pathology SCID pigs possessed concentrations of 2.4, and 3.7 Log10/reaction. Similar results were obtained for BALF. Virus was easily detected and there were no apparent differences between the three groups of pigs. All together, these results demonstrate that PRRSV was present in the lung of all pigs.

PAMs from SCID and WT pigs have similar expression of surface markers

Selection of the population of alveolar macrophages was based on their high side scatter and forward scatter properties on the flow cytometry plot (data not shown). This population of macrophages was then selected or "gated" for further analysis. Figure 4.9 shows the analysis of

the "gated" alveolar macrophages for their expression of CD163, CD172, and SLA II. We investigated the expression of these molecules to confirm the presence of PAMs in the BALF of SCID pigs and to determine the ability of PAMs to permit PRRSV infection. Furthermore, it has been recently proved that CD163 is necessary for permissiveness of PRRSV infection in PAMs and that the lack of this molecule hinders pulmonary pathology in pigs (Prather *et al.* 2013, Whitworth *et al.* 2015). On flow cytometry analysis of PAMs, we demonstrated that both WT and SCID pigs possess a population of $CD163^+/CD172a^+/SLA\text{-}II^+$ macrophages and that there was no significant difference in the expression of these molecules among the groups. This indicates that SCID pig PAMs express normal numbers of CD163, CD172, and SLA-II surface molecules when compared to WT pigs. Although further studies would be necessary to study intracytoplasmic activation of PAMS, our data also indicates that SCID pig PAMs were activated following infection with PRRSV, based on the expression of CD172 and SLA-II. This not only further supports our findings that macrophages in SCID pigs were permissive for infection with PRRSV, but demonstrates their functionality.

Lung lesions in WT pigs are a result of the recruitment and activation of lymphocytes

The interstitial pneumonia observed only in WT pigs in this study is typical of PRRSV infection. In addition, WT pigs had increased numbers of $CD3^+$ T cells around pulmonary blood vessels, a finding consistent with the recruitment of lymphocytes to the inflammatory sites. These findings, along with the presence of similar PRRSV loads in both WT and SCID pigs, suggests that the lung pathology during peak of PRRSV infection is likely the result of the

recruitment and activation of lymphocytes to the interstitial and perivascular areas of the infected lung, and not the sole presence of virus within the lung.

The suppurative pneumonia in two of the SCID pigs was attributed to secondary Gram (+) bacterial infection. Although PRRSV may have contributed to the appearance of the disease in these SCID pigs, we and other had shown that overwhelming bacterial infection is a common outcome of the severe immune depression characteristic of the SCID phenotype in multiple animal species (Pellegrini-Masini *et al.* 2005, Ross *et al.* 1996, Tizzard 2013, Cino-Ozuna *et al.* 2011, Ewen *et al.* 2013). Four of the PRRSV-infected SCID pig did not show evidence of pneumonia. Overall, these findings suggest that bacterial infection only was the cause of the suppurative pneumonia observed in the two other SCID pigs.

SCID pigs as models of T cell functionality during PRRSV infection

The role of PAMs in lung pathology of viral and bacterial infections has been described by several authors. Classically, activation of lung macrophages by viral infection leads to a rapid induction of adaptive immunity in the lung. Kim *et al.* (2008) and Hartwig *et al.* (2014) described the important role of alveolar macrophages for controlling, modulating, and inducing acute lung pathology following infection with influenza virus and murine hepatitis virus-1 (MHV-1), respectively. In a similar way, Knudson *et al.* (2014), Anderson *et al.* (2012), and Khanolkar *et al*. (2009) demonstrated that T cell antigen-specific lymphocytes are recruited to the lung in response to viral infections with multiple viruses, such as lymphocytic choriomeningitis virus (LCMV), respiratory syncytial virus (RSV), influenza A virus, or respiratory coronavirus (MHV-1) in mouse. Similar results were confirmed in pigs infected with

highly pathogenic swine influenza A virus H1N1 (Khatri *et al*. 2010). Following recruitment, T lymphocytes induce lysis of infected cells and inflammation of the tissue through the release of inflammatory cytokines or their cytotoxic activity, as demonstrated by Taylor *et al.* (1985). However, the role of alveolar macrophages or T cells in lung immunopathology after infection with PRRSV is largely unknown. One possible mechanism for PRRSV immunopathology is the direct destruction of alveolar macrophages (Thanawongnuwech *et al.* 1997). Alternatively, a break in the delicate balance of viral protection and excessive activation of T cells in the lung can lead to tissue damage. Overexpression of pro-inflammatory cytokines such as TNF-α and –β, with cytolytic function, or absence of anti-inflammatory cytokines such as IFN-γ or IL-10 can lead to severe lung disease. Expression of TNF-α in swine lymph nodes and lungs (Rowland *et al.* 2001) as well as IFN-γ in lungs of pigs infected with PRRSV at very early infectious stages (Choi *et al.* 2001) was already described. In addition, PRRSV infection has been associated with an immunosuppressive stage attributed to secretion of TGF-β (but not IL-10) by regulatory T cells (Tregs) after *in vitro* PRRSV infection of swine dendritic cells (Silva-Campa, et al. 2009). Thus, we hypothesized that pigs lacking T and B cells were capable of developing severe lung pathology following infection with PRRSV.

Figure 4.10 depicts the major roles of the innate and adaptive immunity following infection of PAMs. Classically, PRRSV infection of PAMs triggers activation of cell-mediated immunity through the presentation of the viral antigen to naïve T cells via MHC class I or II, inciting a $CD8^+$ or a $CD4^+$ T cell response, respectively. Cell mediated immunity then induces lung pathology through the activation of T-cell toxicity and T helper responses. The response and virus load is overall regulated by regulatory T cells (Tregs). In the SCID pig model of PRRSV infection, the absence of lung pathology is a consequence of the lack of $CD4^+$ and $CD8^+$

T cells response. Virus load is elevated due to the absence of regulatory T cells, which through the release of TGF-β regulate the infection of PAMs as well as reduces the response of $CD8^+$ T cytotoxicity.

4.D. Conclusion

The absence of lung pathology in SCID pigs due to PRRSV infection indicates a direct role of T lymphocytes in the pathogenesis of the disease. SCID pig PAMs were permissive to PRRSV replication and expressed similar amounts of $CD163^+$/$CD172^+$/SLA-II^+ markers when compared to WT pigs, which partially indicates permissiveness and functionality of PAMs. These findings suggest a pathogenesis for lung pathology in PRRSV infected pigs as follow: infection of PAMs leads to release of proinflammatory cytokines, which triggers recruitment and activation of $CD4^+$ and $CD8^+$ T lymphocytes and damage to the lung through cytotoxicity and activation of T helper lymphocytes. Due to the lack of T (and B) lymphocytes, this response is absent in SCID pigs, leading to absence of lung pathology. Therefore, SCID pigs are proving to be a good model for the study of T cell functionality during PRRSV infection.

4.E. References

1. Allan, W., Tabi, Z., Cleary, A. & Doherty, P. (1990). Cellular events in the lymph node and lung of mice with influenza, Consequences of depleting CD4+ T cells. *J. Immunol.* 144(10), 3980-3986.

2. Anderson, K. G., Sung, H., Skon, C. N., Lefrancois, L., Deisinger, A., Vezys, V., & Masopust, D. (2012). Intravasuclar staining redefines lung CD8 T cell responses. *J. Immunol.* 189, 2702-2706.

3. Basel, M.T., Balivada, S., Beck, A.P., Kerrigan, M.A., Pyle, M.M., Dekkers, J.C., Wyatt, C.R., Rowland, R.R., Anderson, D.E., Bossmann, S.H., Troyer, D.L., (2012). Human xenografts are not rejected in a naturally occurring immunodeficient porcine line: a human tumor model in pigs. *Biores Open Access* 1(2), 63-68.

4. Boyton R. J. & Openshaw P. J. (2002). Pulmonary defences to acute respiratory infection. *Br. Med. Bull.* 6(1), 1-12.

5. Butler J. E., Zhao Y., Sinkora M., Wertz N., & Kacskovics I. (2009). Immunoglobulins, antibody repertoire and B cell development. *Developmental and Comparative Immunology* 33, 321-333.

6. Chen N., Dekkers J. C. M., Ewen C. L., & Rowland R. R. R. (2014). Porcine reproductive and respiratory syndrome virus replication and quasispecies evolution in pigs that lack adaptive immunity. *Virus Research* 195, 246-249.

7. Chen X., Quan R., Guo X., Gao L., Shi J., & Feng W. (2014). Up-regulation of pro-inflammatory factors by HP-PRRSV infection in microglia: Implications for HP-PRRSV neuropathogenesis. *Veterinary Microbiology* 140, 48-57.

8. Choi, C., Cho, W.-S., Kim, B., & Chae, C. (2001). Expression of interferon-gamma and tumour necrosis factor-alpha in pigs experimentally infected with porcine reproductive and respiratory syndrome virus (PRRSV). *J. Comp. Path.* 127, 106-113.

9. Cino-Ozuna, A.G., Rowland, R.R.R., Nietfeld, J.C., Kerrigan, M.A., Dekkers,J.C., Wyatt, C.R. (2013). Preliminary findings of a previously unrecognized porcine primary immunodeficiency disorder. *Vet. Pathol.* 50,144–146.

10. Costa-Hurtado, M., Olvera, A., Martinez-Moliner, V., Galofré-Milà, N., Martínez, P., Dominguez, J. & Aragon, V. (2013). Changes in macrophage phenotype after infection of pigs with Haemophilus parasuis strains with different levels of virulence. *Infect. Immun.* 81(7), 2327-2333.

11. Costers, S., Lefebvre, D.J., Delputte, P.L., and Nauwynck, H.J. (2008). Porcine reproductive and respiratory syndrome virus modulates apoptosis during replication inalveolar macrophages. *Archives of Virology* 153:1453–1465.

12. Darwich L., Diaz I., and Mateu E. (2010). Certainties, doubts and hypotheses in porcine reproductive and respiratory syndrome virus immunobiology. *Virus Research* 154,123-132.

13. Ewen C. L., Cino-Ozuna A. G., He H., Kerrigan M. A., Dekker J. C. M., Tuggle C. K., Rowland R. R. R., and Wyatt C. R. (2014) Analysis of blood leukocytes in a naturally occurring immunodeficiency of pigs shows the defect is localized to B and T cells. *Veterinary Immunology and Immunopathology* 162, 174-179.

14. Galina L. (1995). Possible mechanisms of viral-bacterial interaction in swine. *Swine Health Production* 3, 9-14.

15. Halbur P. G., Miller L. D., Meng X.-J., Huffman E. L., & Andrews J.J. (1995). Immunohistochemical identification of porcine reproductive and respiratory syndrome virus (PRRSV) antigen in the heart and lymphoid system of three-week-old colostrum-deprived pigs. *Veterinary Pathology* 32,200-204.

16. Halbur P. G., Paul P. S., Frey M. L., Landgraf J., Eernisse K., Meng X.-J., Lum M. A., Andrews J. J., &Rathje JA. (1995). Comparison of the pathogenicity of two US Porcine reproductive and respiratory syndrome virus isolates with that of Lelystad virus. *Veterinary Pathology* 32,648-660.

17. Halbur P. G., Paul P. S., Frey M. L., Landgraf J., Eernisse K., Meng X.-J., Lum M. A., Andrews J. J., & Rathje J. A. (1995). Comparison of the pathogenicity of two US porcine reproductive and respiratory syndrome virus isolates with that of the Lelystad virus. *Veterinary Pathology* 32, 648-660.

18. Hartwig, S. M., Holman, K. M., & Varga, S. M. (2014). Depletion of alveolar macrophages ameliorates virus induced disease following a pulmonary coronavirus infection. *PLos ONE* 9, e90720.

19. Jubb, Kennedy, and Palmer's Pathology of Domestic Animals: volume 2, Chapter 5 - Respiratory. 5th ed. M. Grant Maxie. Elsevier Saunders: Edinburg, 2007.

20. Khanolkar, A., Hartwig, S.M., Haag, B. A., Meyerholz, D. K., Harty, J. T., & Varga, S. M. (2009). Toll-like receptor 4 deficiency increases disease and mortality after mouse hepatitis virus type 1 infection of susceptible C3H mice. *J. Virol.* 83, 8946-8956.

21. Khatri, M., Dwivedi, V., Krakowka, S., Manickam, C., Ali, A., Wang, L., Qin, Z., Renukaradhya, G. J., & Lee, C. W. (2010). Swine influenza H1N1 virus induces acute inflammatory immune responses in pig lungs: a potential animal model for human H1N1 influenza virus. *J. Virol.* 84(21),11210-11218.

22. Kim, H. M., Lee, Y-W., Lee, K-J., Kim, H. S., Cho, S. W., van Rooijen, N., Guan, Y. & Seo, S. H. (2008). Alveolar macrophages are indispensable for controlling influenza viruses in lungs of pigs. *J. Virol*. 82(9), 4265-4274.

23. Knudson, C. J., Weiss, K. A., Hartwig, S. M., & Varga, S. M. (2014). The pulmonary localization of virus-specific T lymphocytes is governed by the tissue tropism of the infection. *J. Virol.* 88, 9010-9016.

24. Lunney J. K., Fritz E. R., Reecy J. M., Kuhar D., Prucnal E., Molina R., Christopher-Hennings J., Zimmerman J., & Rowland R. R. R. (2010). Interleukin-8, interleukin-1β, and interferon-γ levels are linked to PRRS virus clearance. *Viral Immunology* 23(2):127-134.

25. Mateu E. & Diaz I. (2008). The challenge of PRRS immunology. *The Veterinary Journal* 177,345-351.

26. Meier, W. A., Galeota, J., Osorio, F. A., Husmann, R. J., Schnitzlein, W. M., & Zuckermann, F. A. (2002). Gradual development of the interferon-γ response of swine to porcine reproductive and respiratory syndrome virus infection or vaccination. *Virology* 309, 19-31.

27. Ondrackova, P., Leva, L., Kucerova, Z., Vicenova, M., Mensikova, M. & Faldyna, M. (2013). Distribution of porcine monocytes in different lymphoid tissues and the lungs during experimental Actinobacillus pleuropneumoniae infection and the role of chemokines. *Vet. Res.* 44, 98-114.

28. Opriesnig T., Giménez-Lirola L. G. & Halbur P.G. (2011). Polymicrobial respiratory disease in pigs. *Anim. Health Res. Rev.* 12 (2), 133-148.

29. Pellegrini-Masini, A., Bentz, A.I., Johns, I.C, (2005). Common variable immunodeficiency in three horses with presumptive bacterial meningitis. *J. Am. Vet. Med. Assoc.* 221:114-122.

30. Prather, R.S., Rowland, R.R., Ewen, C., Trible, B., Kerrigan, M., Bawa, B., Teson, J.M., Mao, J., Lee, K., Samuel, M.S., Whitworth, K.M., Murphy, C.N., Egen, T., and Green, J.A. (2013) *J. Virol.* 87(17):9538-9546.

31. Pribul, P. K., Harker, J., Wang, B., Wang, H., Tregoning, J. S., Schwarze, J. & Openshaw, P. J. M. (2008). Alveolar macrophages are a major determinant of early responses to viral lung infection but do not influence subsequent disease development. *J. Virol.* 82(9), 4441-4448.

32. Ross, T.L., Balson, G.A., Miners, J.S., Smith, G.D., Shewen, P.E., Prescott, J.F., and Yager, J.A. (1996). Role of CD4+, CD8+, and double negative T-cells in the protection of SCID/beige mice against respiratory challenge with Rhodococcus equi. *Can. J. Vet. Res.* 60:186

33. Rowland, R. R., Robinson, B., Stefanick, J., Kim, T. S., Guanghua, L., Lawson, S. R., & Benfield, D. A. (2001). Inhibition of porcine reproductive and respiratory syndrome virus by interferon-gamma and recovery of virus replication with 2-aminopurine. *Arch. Virol.* 146, 539–555.

34. Silva-Campa, E., Flores-Mendoza, L., Reséndiz, M., Pinelli-Saavedra, A., Mata-Haro, V., Mwangi, W., & Hernández, J. (2009). Induction of T helper 3 regulatory cells by dendritic cells infected with porcine reproductive and respiratory síndrome virus. *Virology* 387, 373-379.

35. Tate, M. D., Pickett, D. L., van Rooijen N., Brooks, A. G., Reading, P.C. (2010). Critical role of airway macrophages in modulating disease severity during influenza virus infection of mice. *J. Virol.* 84(15), 7569-7580.

36. Taylor, G., Stott, E. J., & Hayle, A.J. (1985). Cytotoxic lymphocytes in the lungs of mice infected with respiratory syncytial virus. *J. Gen. Virol.* 66, 2533-2538.

37. Thanawongnuwech, R., Thacker, E. L., & Halbur, P. G. (1997). Effect of porcine reproductive and respiratory syndrome virus (PRRSV) (isolate ATCC VR-2385) infection on bactericidal activity of porcine pulmonary intravascular macrophages (PIMs): in vitro comparisons with pulmonary alveolar macrophages (PAMs). *Vet. Immunol. Immunopathol* 59, 323-335.

38. Tizard, I.R., Veterinary Immmunology: Chapter 37 – Primary immunodeficiencies. 9th ed. Elsevier Saunders: St. Louis, Missouri, 2013.

39. Whitworth, K.M., Rowland, R.R., Ewen, C.L., Trible, B.R., Kerrigan, M.A., Cino-Ozuna, A.G., Samuel, M.S., Lightner, J.E., McLaren, D.G., Mileham, A.J., Wells, K.D., and Prather, R.S. (2015). Gene-edited pigs are protected from porcine reproductive and respiratory syndrome virus. *Nature Biotechnology* (available online).

40. Yap, K. L., Ada, G. L. & McKenzie, I. F. C. (1978). Transfer of specific cytotoxic T lymphocytes protects mice inoculated with influenza virus. *Nature* 273, 238-239

41. Zhang L., Liu J., Bai J., Wang X., Li Y., & Jiang P. (2013). Comparative expression of Toll-like receptors and inflammatory cytokines in pigs infected with different virulent porcine reproductive and respiratory syndrome virus isolates. *Virology Journal* 10, 135-145.

Tables and Figures

Figure 4.1 Outline of the study.

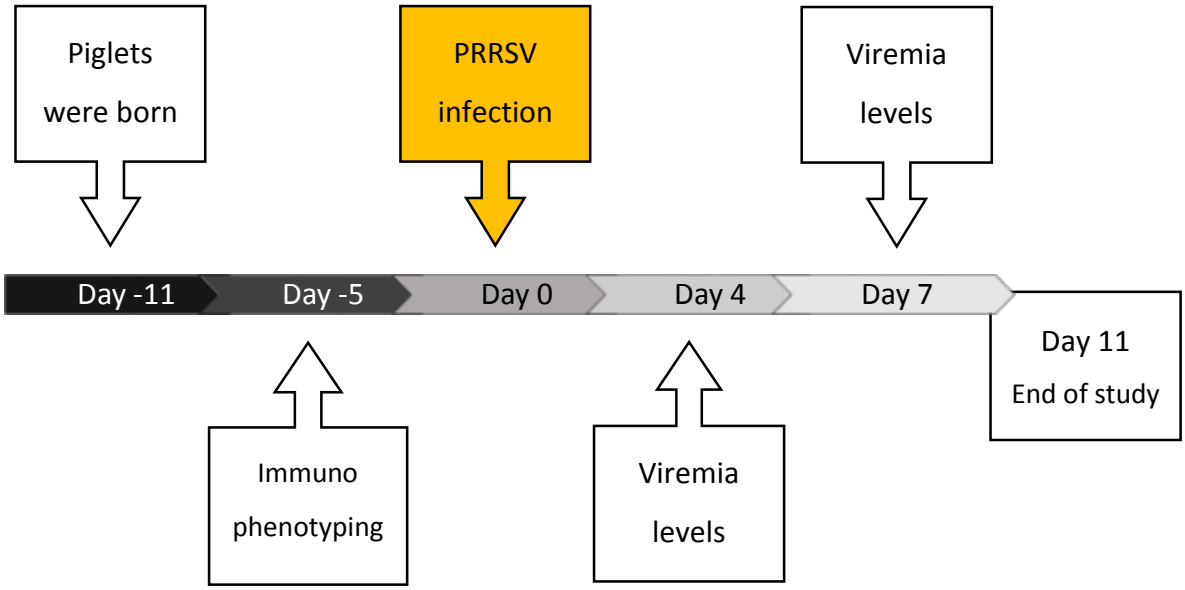

Figure 4.2 Location of lymphocytes in leukocytes from whole blood.

Upper panels show forward scatter (FS) and side scatter (SS) properties of leukocytes from whole blood. The red area shows the location of lymphocytes. The bottom panels show that the T cell population is located within the lymphocyte gate. The lymphocyte population in SCID pigs is dominated by NK cells (see Table 4.3).

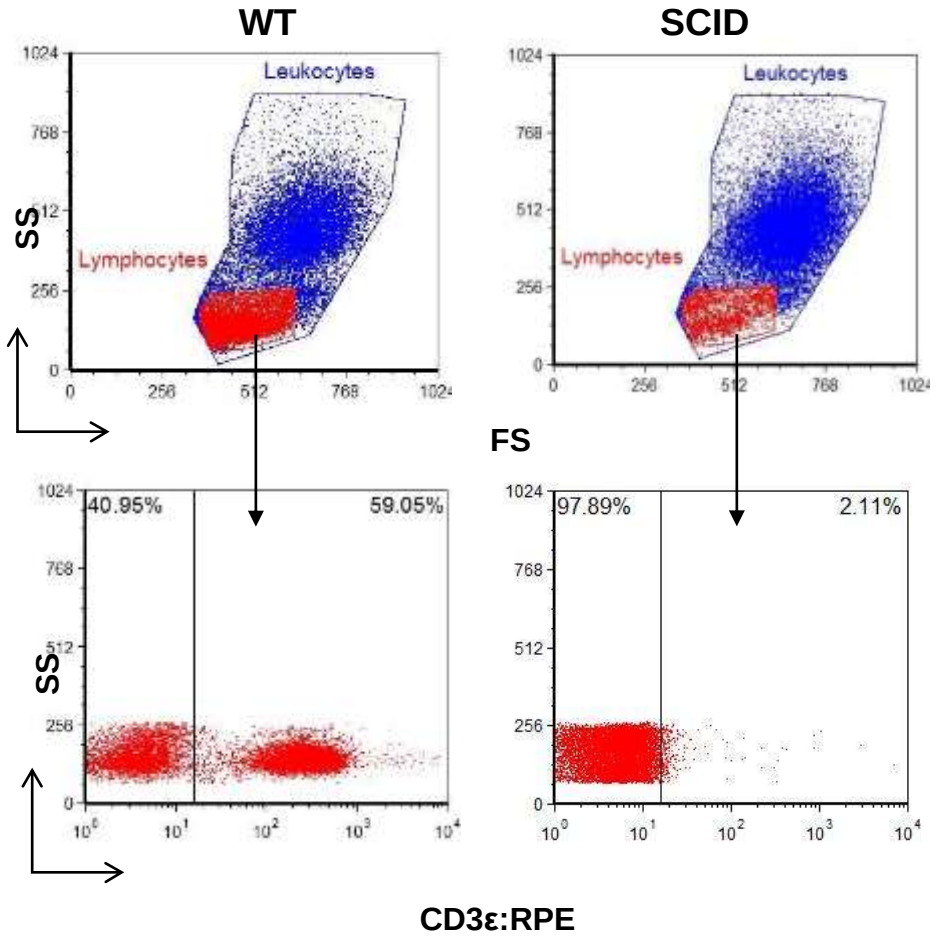

Figure 4.3 (Video) Clinical signs of WT pig at 10-days post-infection with PRRSV

The animal shows an overall poor body condition and has an increased respiratory rate and effort. The head is down and the eyes are swollen and watery, indicating systemic illness. (Click in this link to watch the video).

Figure 4.4 Gross image of lung from PRRSV-infected WT pig at day 10 post-infection.
The lung is diffusely congested and edematous and contains multifocal to coalescing areas of hemorrhage and pneumonia, consistent with interstitial pneumonia characteristic of PRRSV infection.

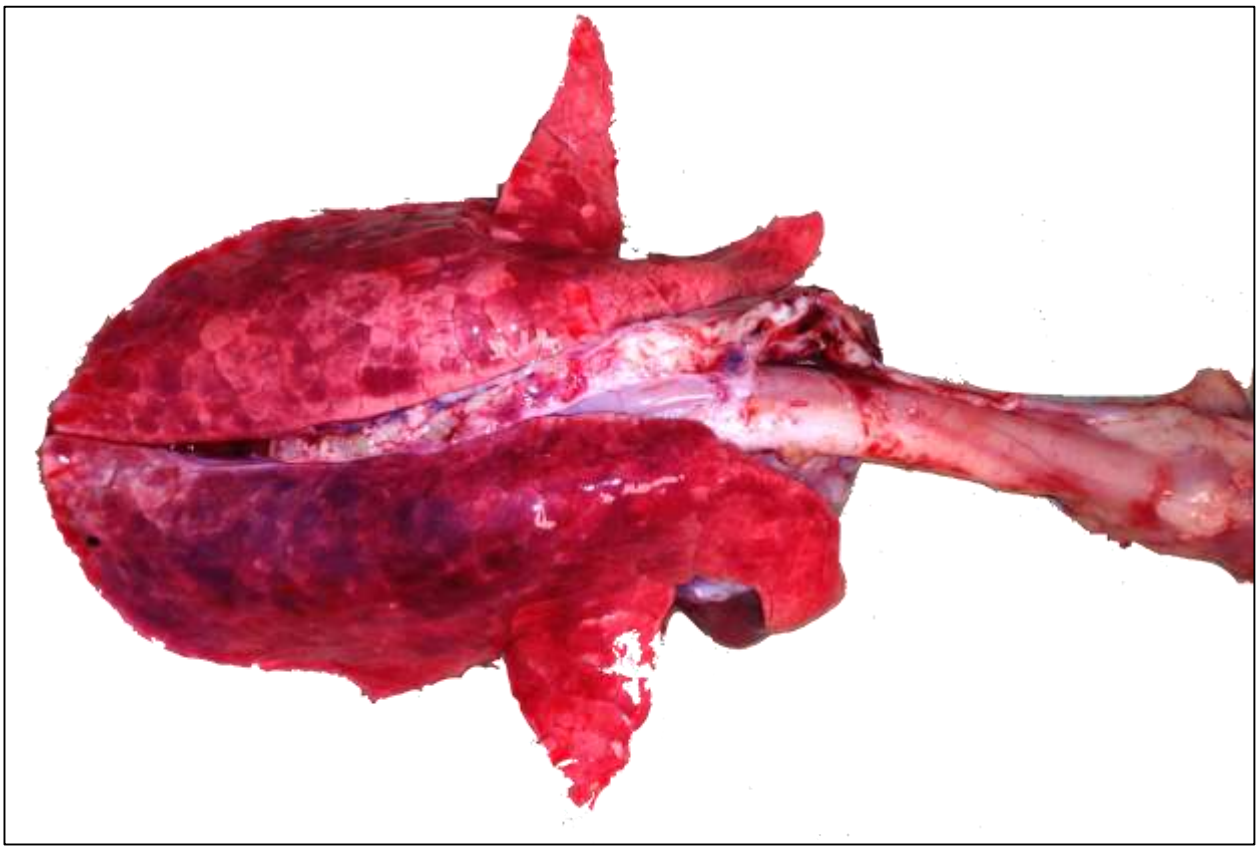

Figure 4.5 Photomicrographs of lung tissue from PRRSV-infected WT and SCID pigs at day 10 post-infection

Insert shows anti-CD3 IHC staining for T cells. A. Lung from a non-infected age-matched normal pig. B. Lung from a representative PRRSV-infected WT pig. C. Lung from a representative PRRSV-infected SCID pig with no pulmonary lesions. D. Lung from a PRRSV infected SCID pig with bacteria-associated suppurative pneumonia. All large micrographs are 20x and insert micrographs 20x. Arrows identify the location of blood vessels.

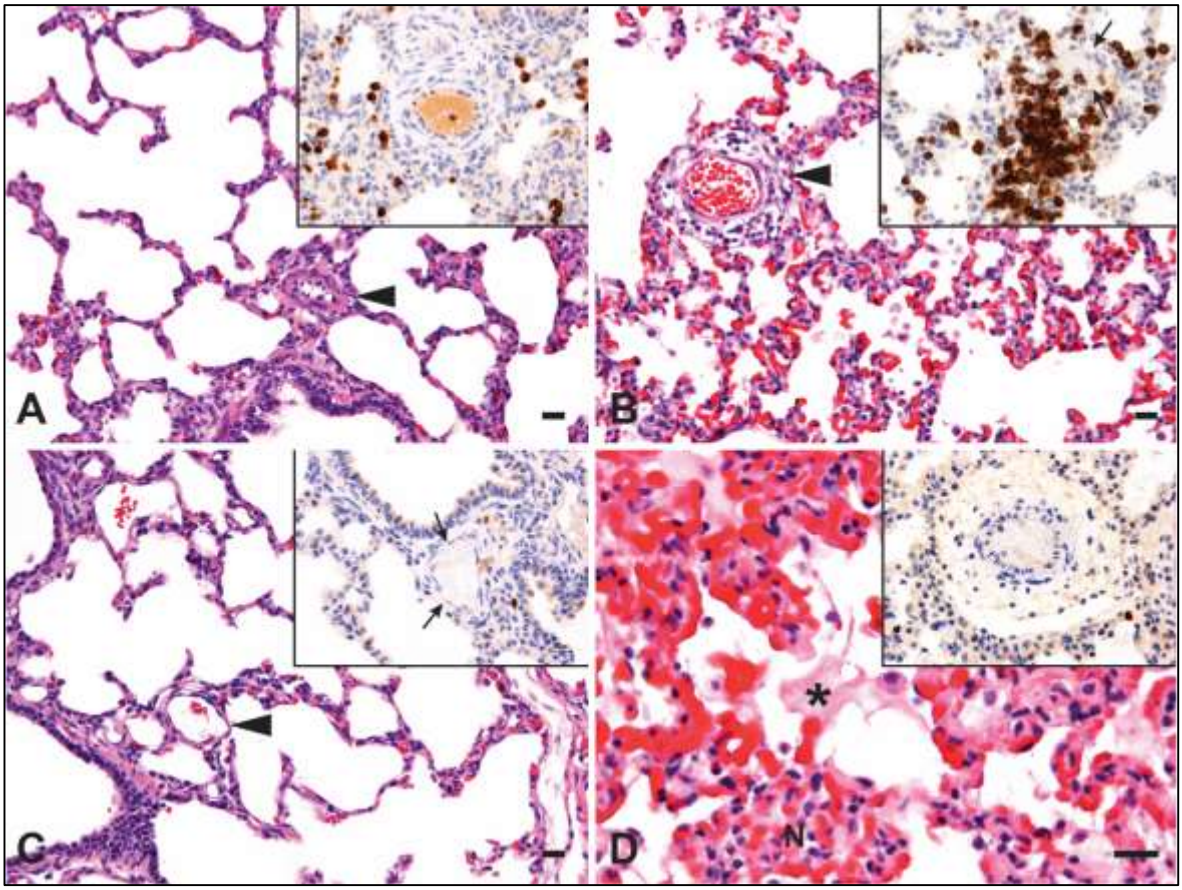

Figure 4.6 Gram staining of WT lung at 10 days after infection with PRRSV.

The arrow points to a mononuclear cell with numerous Gram positive bacteria (stained in blue) within the cytoplasm. Gram staining, magnification 60X.

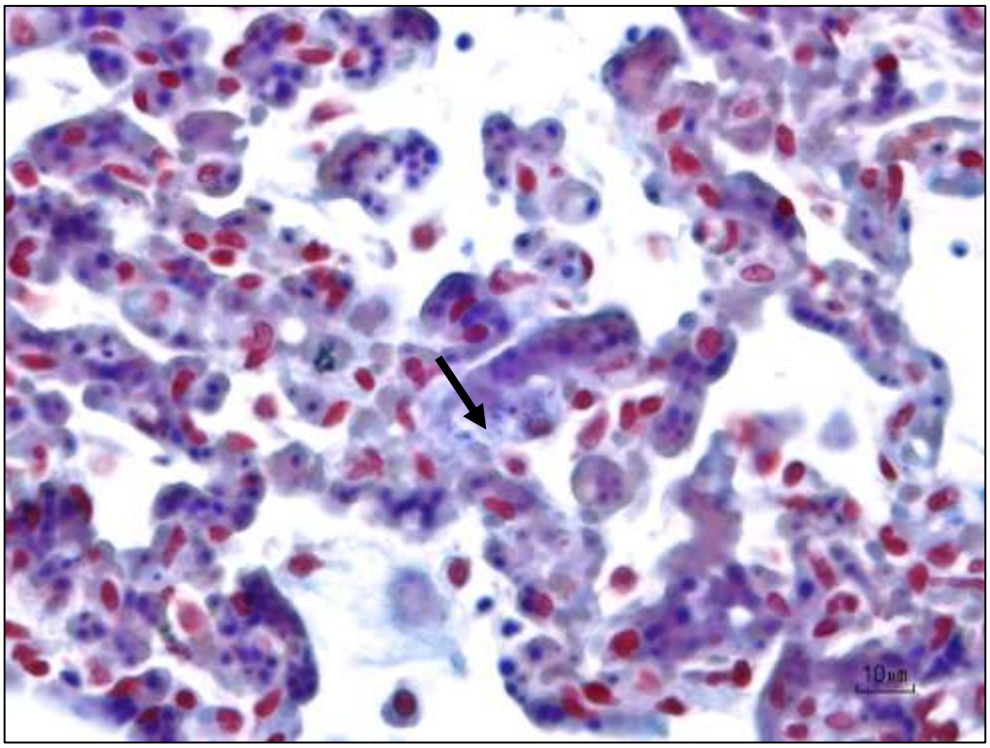

Figure 4.7 PRRSV nucleic acid in serum, BALF and PAMs at10 days after infection with PRRSV.

The horizontal lines identify the mean value for each group.

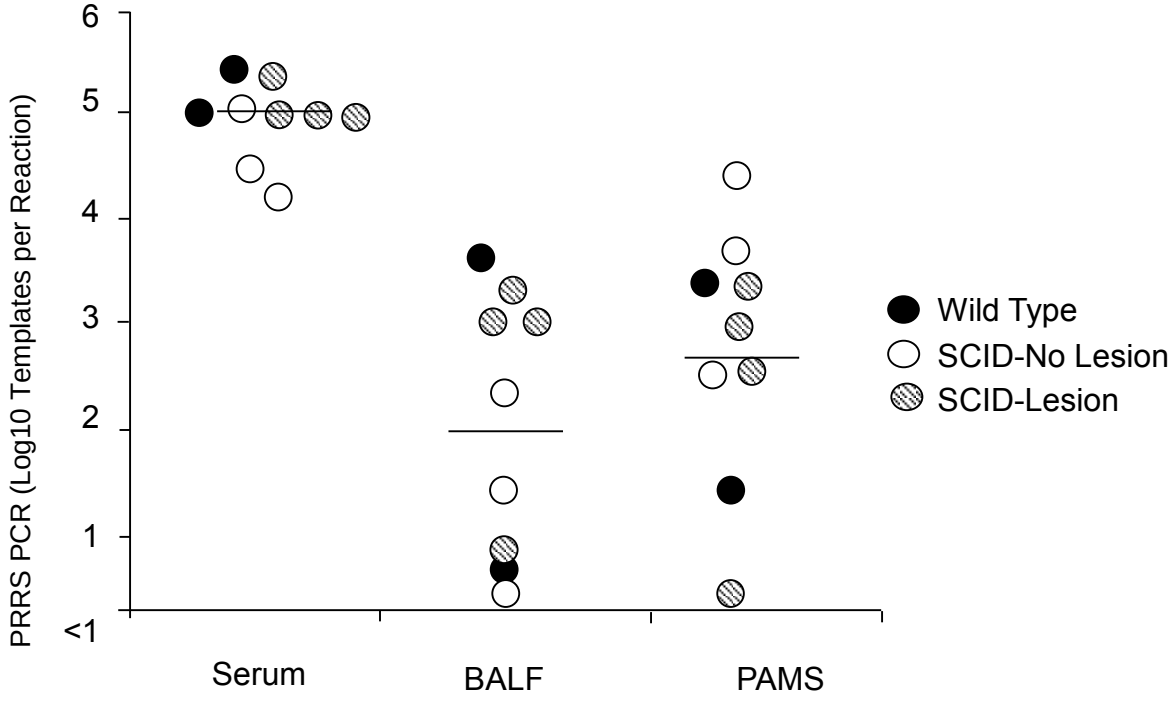

Figure 4.8 Comparison of viremia levels on WT and SCID pigs at 10-days after PRRSV infection.

No significant differences were observed in the viremia levels between WT and SCID pigs. (Student's T test).

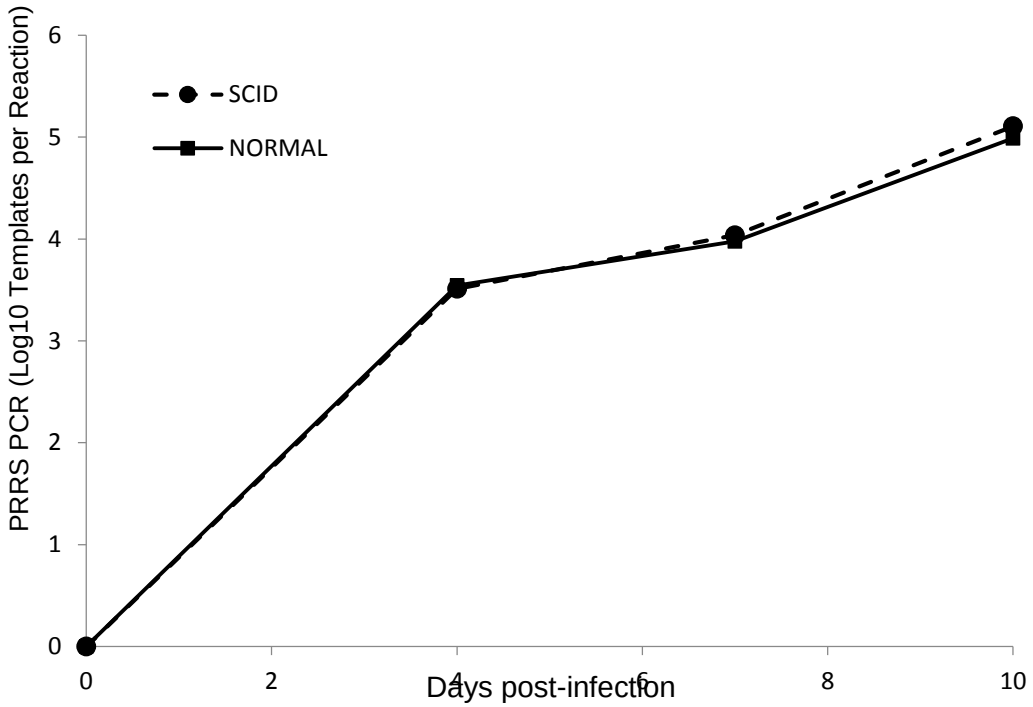

Figure 4.9 Flow cytometry results of PAMs at 10 days after PRRSV infection.

Panel A shows representative results from wild type pigs. The left dot plot shows the position and gating of $CD172^+$ and $CD163^+$ alveolar macrophages. The histogram on the right represents the expression of SLA-II (red line) on $CD172^+/CD163^+$ population of macrophages. The black line on the histogram represents the isotype control.

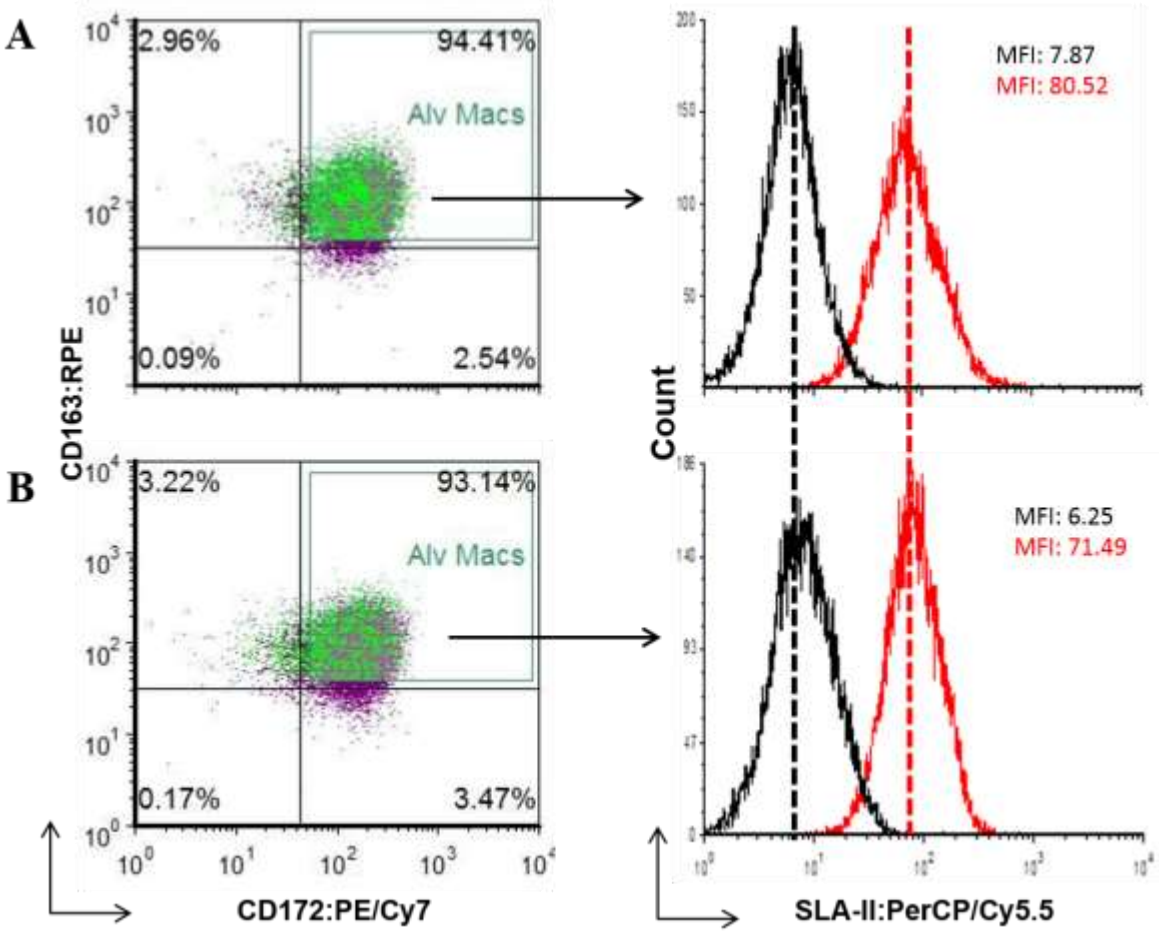

Figure 4.10 SCID pig model of PRRSV infection

The figure depicts the major roles of the innate and adaptive immunity during PRRSV infection in wild-type pigs. Classically, PRRSV infection of porcine alveolar macrophages (PAMs) triggers activation of cell-mediated immunity through the presentation of the viral antigen to naïve T cells via MHC class I or II, inciting a CD8 or a CD4 T cell response, respectively. Cell mediated immunity then induces lung pathology through the activation of T-cell toxicity and T helper responses. The response and virus load is overall regulated by regulatory T cells (Tregs). In the SCID pig model of PRRSV infection, the absence of lung pathology is a consequence of the lack of CD4 and CD8 T cells response. Virus load is elevated due to the absence of regulatory T cells.

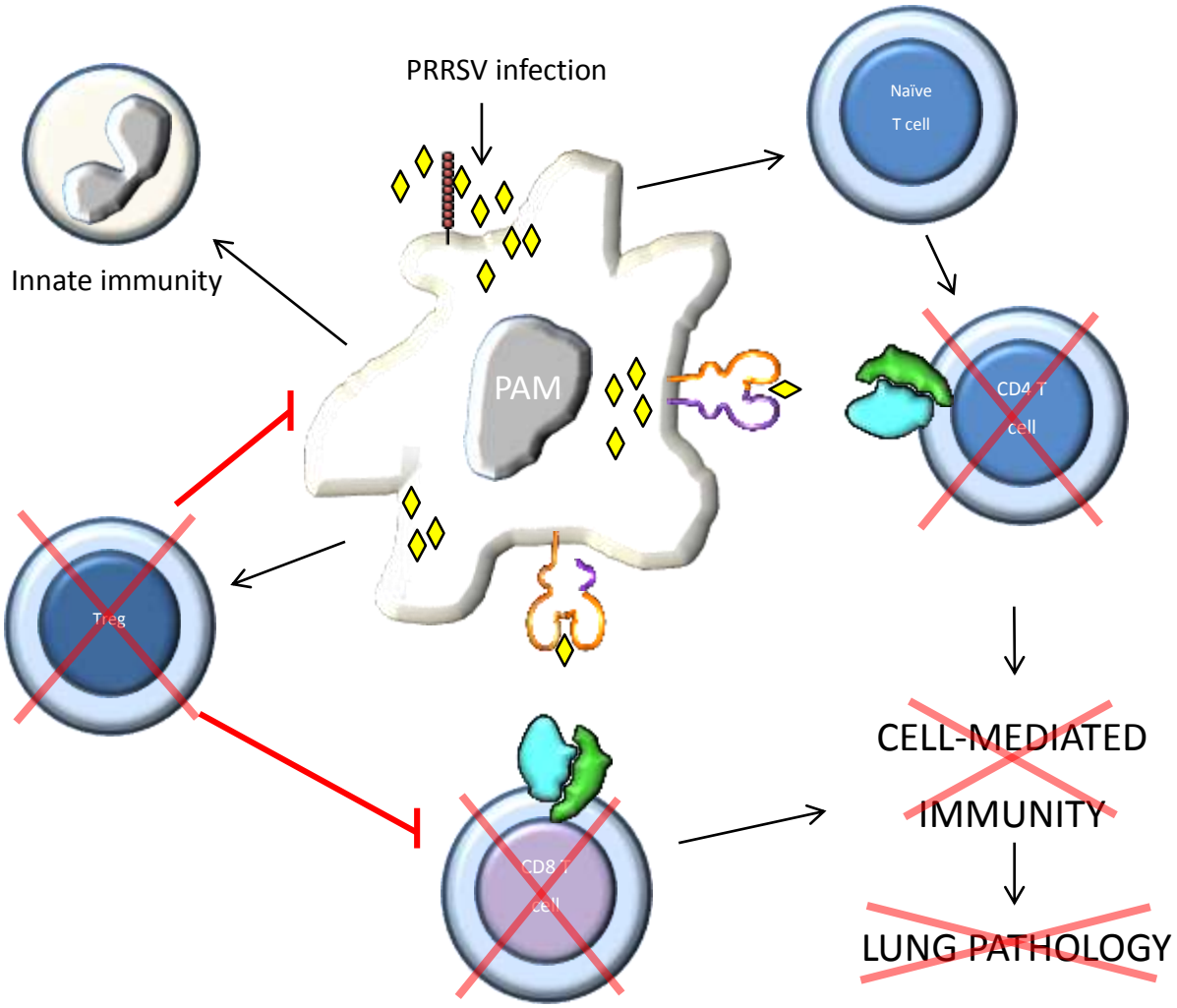

Table 4.1 Primary and secondary antibodies to immunophenotype blood leukocytes in flow cytometry.

Blood leukocytes

Primary antibody	**Fluorochrome**	**Clone**
CD3ε	R-phycoerythrin (R-PE)	PPT3
CD4	Fluorescein isothiocyanate (FITC)	74-12-4
CD8α	Phycoerythrin (P-Cy5E)	76-2-11
CD14	Pacific Blue (PB)	TÜK4
CD16	FITC	G7
CD21	Allophycocyanin (APC)	BioBB6-11C9
γδ T cell	--(Isotype IgG1)	PGBL22A
FoxP3	R-phycoerythrin-Cyanine 7 (PE/Cy®7)	FJK-16s
Secondary antibody	**Fluorochrome**	**Clone**
IgG1	Brilliant violet 421 (BV421)	RMG1-1

Table 4.2 Primary and secondary antibodies for porcine alveolar macrophages (PAMs) in flow cytometry.

Pulmonary alveolar macrophages

Primary antibody	**Fluorochrome**	**Clone**
CD163	R-PE	2A10/11
CD172α	No fluorochrome (IgG2b)	74-22-15A
MHC-II (SLA-II)	No fluorochrome (IgG2a)	MSA II
Secondary antibody	**Fluorochrome**	**Clone**
IgG2a	Peridinin-chlorophyll proteins/Cyanine 5.5 (PerCP/Cy®5.5)	RMG2a-62
IgG2b	PE/Cy®7	--

Table 4.3 Leukocyte immunophenotyping at two days after birth

Pig#	Granulocytes (cells/µl)	Lymphocytes (cells/µl)			
		Total	$CD3^+$	$CD21^+$	$CD16^+$
Wild-Type					
1	1277	1168	754	114	75
6	1516	1372	802	252	93
Mean	1387	1270	778	183	84
SCID					
2	1387	105	3	0	65
3	2794	754	50	1	385
4	1659	216	13	1	83
7	981	135	16	0	53
8	1320	152	15	0	94
9	2113	154	9	0	70
11	2284	562	18	0	303
Mean	1791±634	297±255	17±15	0±0	150±134

* Absolute granulocyte and total lymphocyte counts were obtained by flow cytometry based on side and forward scatter plots. Whole blood was stained with mouse anti-pig CD3ε-RPE (T lymphocyte marker), mouse anti-pig CD21-APC (B lymphocyte marker), and mouse anti-pig CD16-RPE (NK cell marker) for immunophenotyping of lymphocyte populations.

Chapter 5 - Adoptive transfer of purified $CD3^+$ T cells into a naturally occurring line of SCID pigs results in engraftment of full T cell subsets

Abstract

We examined two different protocols for the ability to engraft purified $CD3^+$ T lymphocytes into receptor SCID pigs from SLA II-matched wild type donor littermates. The first protocol (experiment A) included the adoptive transfer of purified $CD3^+$ T lymphocytes obtained from spleen, lymph nodes, and whole blood. The second protocol (experiment B) included the adoptive transfer of purified thymocytes. In both experiments, adoptive transfer was performed via intravenous injection of a suspension of purified $CD3^+$ T cells into the cranial vena cava of the receptor SCID pigs at approximately 10 days of age. Engraftment was monitored for 27 days (experiment A) and 49 days (experiment B) post adoptive transfer by flow cytometry analysis of peripheral blood mononuclear cells using antibodies for $CD3^+$ T cells. No engraftment of $CD3^+$ T lymphocytes was observed in experiment A. However, engraftment of $CD3^+$ T cells was observed in experiment B starting at day 28-post adoptive transfer, and was characterized by increased numbers of lymphocytes in whole blood and in lymphoid tissues. Engraftment was confirmed by immunohistochemistry by day 49 post-transfer. Immunophenotyping of T cell subsets at the end of the study revealed engraftment of full repertoire of T cell populations in the experiment B. This protocol describes the first engraftment of purified T cells into SCID pigs and could provide a foundation for studies of T cell immunobiology on infectious diseases.

5.A. Introduction

Severe combined immunodeficiency (SCID) is a group of disorders of the immune system characterized by the lack of adaptive immunity, with defects in both T and B lymphocytes (Notarangelo *et al.* 2010). Naturally occurring SCID has been described in humans and several animal species, including CB.17 mice, Jack Russell Terrier dogs, Arabian foals, and more recently in a line of partially inbred Yorkshire pigs that were bred for feed efficiency (Blunt *et al.* 1995, Danska *et al.* 1996, Meek *et al.* 2001, Bell *et al.* 2002, Cino-Ozuna *et al.* 2013). SCID pigs are characterized by hypoplastic primary and secondary lymphoid follicles due to nearly total absence of T and B lymphocytes, failure to produce antibodies following viral infection (Cino-Ozuna *et al.* 2013), and failed to reject human tumor cells (Basel *et al.* 2012). Ewen *et al.* (2014) reported that the defect of these pigs is located in the B and T cells, but SCID pigs have normal numbers of circulating NK cells, neutrophils, and monocytes. This phenotypic appearance is due to a couple of mutations in the *Artemis* gene (Waide *et al.* 2015), a novel discover that differs from the widely recognized mutation in DNA PKcs reported in our veterinary species (Notarangelo *et al.* 2010, Meek *et al.* 2001, Danska *et al.* 1996, Blunt *et al.* 1995).

Numerous characteristics of the swine species, including size, number of piglets/litter, longevity, and relatively low cost of maintenance, place the pigs as a valuable biomedical model. In addition, recent findings in macrophage functions, mucosal immunologic responses, and inflammation in pigs have demonstrated that this species has more similarities to humans than the widely used murine model (Meurens *et al.* 2012, Mair *et al.* 2014). Due to these similarities, there is an increasing interest in developing porcine models and this has been possible due to the remarkable advances in genomic sequence and molecular biology, making the generation of

transgenic and knockout pig lines a reality. As examples, new pig lines with SCID phenotype, either targeting the *RAG1/2* or *Il2rg* genes, were created in the last few years (Suzuki *et al.* 2012, Ito *et al.* 2014), and only bone marrow reconstitution was reported to date (Suzuki *et al.* 2012). Reconstitution of purified $CD3^+$ T cells has not yet been attempted in porcine species, to date.

PRRSV is the most devastating viral disease in the swine industry with enormous economic losses. The exact pathogenesis of the disease and the role of the adaptive immunity during PRRSV infection are not completely understood. Therefore, there is an urgent need for the development of a swine model to study the immunopathogenesis of PRRSV, and more specifically, to further investigate the contribution of T lymphocytes in the pathology and immunity against PRRSV infection. In a previous study, we demonstrated that SCID pigs were permissive to replication of porcine reproductive and respiratory syndrome virus (PRRSV) in pulmonary alveolar macrophages (PAMs), but did not develop lung lesions typical of PRRSV infection (data not published), which suggested a major role of T cells in the developing of lesions during PRRSV infection.

The objective of this study was to establish a model of reconstitution of $CD3^+$ T cells on the recently described naturally occurring SCID pig model (Cino-Ozuna *et al.* 2013). Due to the lack of B cells in this SCID porcine model, selective reconstitution of T cells would allow the study of the biological response of $CD3^+$ T cells and their subsets during viral infections, and could potentially be used as a model of adaptive cellular immunity in studies of cancer, transplantation, and autoimmune diseases. In addition, this reconstitution model seeks to serve as a standard for adoptive transfer of other selective cell lines into the SCID pigs.

5. B. Materials and methods

Animals and experimental design

The animal experiments were performed in accordance with the Federation of Animal Science Societies (FASS) Guide for the Care and Use of Agricultural Animals in Research and Teaching and the USDA Animal Welfare Act and Animal Welfare Regulations, and were approved by the Kansas State University institutional animal care and biosafety committees. Pigs were obtained from the cross of an immunocompetent heterozygous SCID +/- dam with a homozygous recessive SCID boar that was reconstituted with bone marrow cells from a wild type (WT) littermate, as previously described (Cino-Ozuna *et al.* 2013). Animals were housed at the Large Animal Research Center (LARC), at Kansas State University. Genetically matched littermates were identified from blood samples submitted to Dr. Sam Ho, at the Gift of Life Michigan (Ann Arbor, MI) for complete SLA II-typing (Ho *et al*. 2009, Ho *et al*. 2010). Pigs from two different litters, A and B, were used for the experiments, as described below.

- Litter A was comprised of a total of 8 piglets, 3 of which with SCID and 5 WT littermates.
- Litter B was comprised 13 piglets, seven with SCID phenotype and 6 WT (Table 5.1).

Two experiments (Experiment A and B, using pigs from litter A and B, respectively) were designed with the purpose of establishing a model of engraftment of purified $CD3^{+}$T lymphocytes from WT pigs in SCID littermates. In both experiments, adoptive transfer of $CD3^{+}$T cells was performed following SLA-II matching of WT and SCID pigs and, when possible, gender matching. Figure 4.1 shows the outline of the two experiments. In both

experiments, immunophenotyping was performed at 2 days after birth (day -8) and adoptive transfer was performed at 10 days after birth (day 0 of the experiments).

Immunophenotyping for recognition of SCID in pigs

The presence of the SCID phenotype in each piglet was determined by flow cytometry analysis on whole blood taken at two days after birth, and the results were similar to the ones observed by Ewen *et al*, 2014. Briefly, 100 µl of whole blood was placed in FACS tubes and stained with 50 µl of a solution containing the primary antibodies in PBS (concentration 1:20). Primary antibodies (Table 4.2) include R-phycoerythrin (RPE)-conjugate mouse anti-pig CD3ε (clone BB23-8E6, SouthernBiotech, Birmingham, AL, USA), allophycocyanin (APC)-conjugate mouse anti-pig CD21 (clone B-ly4, BD Pharmingen™, San Jose, CA, USA), and fluorescein isothiocyanate (FITC)-conjugate mouse anti-pig CD16 (clone G7, AbD Serotec, Raleigh, NC, USA). Red blood cells were lysed using RBC Lysis Buffer™ (eBioscience, Inc. San Diego, CA USA). A total of 100,000 white blood cells were collected and analyzed on EC800 flow cytometer (Sony Biotechnology, Champaign, IL, USA) and FCS Express 4 software (De Novo Software, Glendale, CA, USA).

Isolation and purification of $CD3^+$ T lymphocytes via cell sorting

Necropsy of WT SLA II-matched donor pigs was performed on a biosafety cabinet using caution to avoid contamination of tissues at approximately 10 days of age.

- For Experiment A: Spleen, lymph node, and whole blood were obtained from WT SLA II-matched pigs and processed routinely in the immunology lab to isolate

peripheral lymphocytes. For spleen and lymph nodes, tissues were harvested from SLA II-matched donor pigs and connetive tissue was removed. Tissues were cut into pieces ≤ 2 cm^2 with a scalpel and placed in digestion media that contained collagenase I (Thermo Scientific) for 30-45 minutes with agitation. Cells in suspension were then filtered through a 100 μM nylon mesh. An additional red blood cell lysis step was done for the spleen, 10x RBC Lysis Buffer (Multi-species, cat # 00-4300-54). Cells were then washed in PBS for cell counting and viability assessment and prepared at a concentration of 2×10^7 cells / mL. For whole blood, peripheral blood mononuclear cells (PBMCs) were obtained by gradient separation using Ficoll-Paque Plus (GE Healthcare Life Sciences, Pittsburg, USA). PBMCs were then suspended in PBS for cell counting and viability assessment and were resuspended at 2×10^7 cells / mL.

- For experiment B: T lymphocytes (thymocytes) were obtained exclusively from the thymus. Thymus tissue was excised from SLA-matched normal donor littermates, and trimmed of any connective tissue. Tissues were cut into ≤ 2 cm^2 pieces using a scalpel, then placed in media containing 100 U/ml collagenase I (Thermo Scientific) for 1 hour, with agitation. The resulting cell suspension was filtered through a 100 μM nylon mesh, washed with PBS, counted and prepared at a concentration of 1- 8 $x10^8$ cells / mL in ice-cold, sterile PBS.

The lymphocytes obtained after tissue processing were stained with CD3ε-R-PE antibody (clone BB23-8E6, SouthernBiotech, Birmingham, AL, USA) at a concentration of 4 μl/$1x10^6$ cells. $CD3^+$ T lymphocytes were sorted using a MoFlo™ cell sorter (Beckman Coulter, Indianapolis, IN, USA). Approximately 1 mL of cell suspension was drawn into a 3mL syringe

(BD, USA), and transported on ice to the LARC. The adoptive transfer was performed by injection of the purified CD3+ T lymphocytes into the cranial vena cava of SLA II-matched recipient SCID pig at approximately 10 days after birth, using a 23G X 1" SafetyGlide Needle (BD, Franklin Lakes, NJ).

Immunophenotyping of CD3$^+$ T cell subsets in blood and tissues

Evaluation of CD3$^+$ T cell engraftment was performed on peripheral blood at days 12 and 27 post adoptive transfer for experiment A and at days 16, 35, and 49 post adoptive transfer for experiment B (See Figure 5.1). Whole blood was obtained from cranial vena cava and PBMCs were stained with primary and secondary antibodies as described above.

The following antibodies were used for flow cytometric analysis of PBMCs (see Table 5.2): R-phycoerythrin (R-PE) mouse anti-pig CD3ε (clone BB23-8E6, Southern Biotech, Birmingham, AL), Fluorescein isothiocyanate (FITC) mouse anti-porcine CD4α (clone 74-12-4, Southern Biotech, Birmingham, AL), and Phycoerythrin-Cyanine 5 (PE-Cy5®) anti-CD8α (clone 76-2-11, Southern Biotech, Birmingham, AL). Antibodies to porcine γδ (clone PGBL22A, IgG1), and anti-CD25 (clone PGBL25A, IgG1) were from Washington State University (Pullman, WA). Intreacellular staining for porcine FoxP3 was performed with R-phycoerythrin-Cyanine 7 (PE/Cy®7) rat anti-porcine FoxP3 (clone FJK-16s, Affymetrix/eBioscience, San Diego, CA). Anti-porcine CD21 (clone B-ly4) was from BD Biosciences (San Jose, CA), and anti-CD14 (clone TUK4) and anti-CD16 (clone G7) antibodies were from AbD Serotec (Raleigh, NC). For secondary antibody, detection antibody BV-421 conjugated rat anti-mouse IgG1 was from BioLegend (clone RMG1-1; San Diego, CA).

Two separate multiparametric staining protocols were developed, containing each FoxP3 and CD25 primary antibodies, since these antibodies were not labeled with fluorochromes and both had the same immunoglobulin subclass (IgG1). IgG1 subclass was detected with the secondary detection antibody BV-421. Briefly, primary antibodies were added to the cell suspension, incubated at room temperature for 30 minutes, and washed twice with PBS.

For CD25 staining, an additional incubation period with the secondary detection antibody (BV-421) for 30 minutes at room temperature was performed. Cells were then washed twice with PBS prior to acquisition.

For FoxP3 intracellular staining, cells were initially surface stained with the primary antibodies, then fixed with 1x Fixation Buffer (FoxP3 staining buffer kit; Affymetrix/eBioscience, San Diego, CA) for 35 minutes at room temperature. Following washes, and permeabilization with 1x FoxP3 Permeabilization Buffer according to manufacturing instructions, anti-FoxP3 or an isotype control antibodies were added to cells for 30 minutes, then washed twice more with 1x FoxP3 Permeabilization Buffer prior to acquisition.

Peripheral blood mononuclear cells were acquired and analyzed, respectively, on EC800 flow cytometer (Sony Biotechnology, Champaign, IL, USA) and FCS Express 4 software (De Novo Software, Glendale, CA, USA).

For the total lymphocyte cell counts, a gate was placed in the lymphocyte population on the forward and side scatter plots, as previously described (Ewen *et al.* 2014). For percentages of $CD3^+$ T and $CD21^+$ B lymphocytes, a plot comparing both parameters was created. Within this plot, the $CD3^+$ T cell population was then selected (gated) and this population was then analyzed for the different subsets of lymphocytes. Lymphocytes that were gated on the $CD4^+CD3^+$ population, were furtherly analyzed for $CD25^+$ and $FoxP3^+$ specific staining.

Histopathology and immunohistochemistry

Sections from all the primary and secondary lymphoid tissues, including thymus, spleen, submandibular lymph node, tracheobronchial lymph node, inguinal lymph node, mesenteric lymph node, ileal Peyer's patches, tonsil, as well as other tissues were harvested from WT and SCID pigs and immediately fixed in 10% buffered formalin, processed for sectioning, and stained with hematoxylin and eosin (H&E). Immunohistochemistry (IHC) staining for T lymphocytes and B lymphocytes was done in all the tissues using an automated IHC staining procedure performed by the Kansas State Veterinary Diagnostic Laboratory. T cells were stained with T cell-specific mouse anti-human CD3ε monoclonal antibody (clone LN10, Leica Biosystems, Buffalo Groove, IL, USA), which is specific for the non-glycosylated epsilon chain of the CD3 molecule. B-cell specific mouse anti-human CD79a monoclonal antibody (clone HM57, Abcam, Cambridge, MA, USA). Antibody was added to the slide following heat-induced epitope retrieval to expose antigen epitopes and allow the binding of antibodies to the target. Bound antibody was detected with biotinylated goat anti-rabbit or anti-mouse immunoglobulin, followed by DAB chromogen (Leica Biosystems, Buffalo Groove, IL, USA). Slides were counterstained with hematoxylin.

5.C. Results and discussion

$CD3^+$T lymphocytes in peripheral blood

Animals were evaluated by flow cytometry three days after birth for the presence of B and T cells in peripheral blood. Concentrations of $CD3^+$ T lymphocytes and $CD21^+$ B lymphocytes per µL of whole blood were calculated; WT pigs contained a mean of 233 $CD3^+$ T cells/ µL (N = 6; S.D. = 45.74) and a mean frequency of 76.62% of lymphocytes, while pigs possessing the SCID phenotype averaged 1.5 CD3+ T cells/ µL (N=8; S.D. = 1.01), and a mean of 4.5% of lymphocytes. WT pigs contained an average concentration of 20 $CD21^+$ B cells/ µL (6.7% of lymphocytes), while pigs affected with SCID averaged 0.05 $CD21^+$ B cells/ µL (0.17% of lymphocytes, see Figure 5.2).

Engraftment of $CD3^+$ T lymphocytes was assessed in both experiments measuring the number of $CD3^+$ cells in peripheral blood at different stages. For experiment A, whole blood was obtained at days 12 post adoptive transfer and at the end of the experiment, on day 27 post adoptive transfer. Results from that experiment showed no significant increase in the number of lymphocytes in peripheral blood at those times and we concluded that there was no $CD3^+$ T lymphocyte engraftment on these pigs.

For Experiment B, blood was obtained at days 16 and 35 post adoptive transfer, and at the end of the study, on day 49 post adoptive transfer. Figure 5.3 shows the representative numbers of $CD3^+$ T lymphocytes in peripheral blood at days -9, +16, +35, and +49 post-adoptive transfer. At day 16 post adoptive transfer, peripheral blood was collected from normal, non reconstituted SCID (SCID-non recon), and reconstituted SCID (SCID recon) piglets, and monitored by flow cytometry for the engraftment of T cells. In SCID-recon pigs, the mean $CD3^+$ T cell lymphocyte concentration was 29.3 cells/ µL (S.D. = 14.3; N=3), ranging from 8.44% to

27.44 % of lymphocytes, while untreated SCIDs remained <3 cells/µL of blood and <4% of lymphocytes (N=3). By day 35 post adoptive transfer, the concentration of $CD3^+$ T cells in SCID-recon increased to a mean of 318 T cells/ uL (N=3; S.D. = 501.97) and ranged from 13.9% to 46.6% of lymphocytes, while SCID-non recon controls averaged 12 cells/ uL (N=3; S.D. = 2.7) and averaged of 4.5% of lymphocytes. By day 49 post adoptive transfer, levels of CD3+ cells in SCID-recon had significantly increased to a mean of 795.69 T cells/ uL blood (N=3; S.D. = 531) and ranged from 59.36% to 68.95% of lymphocytes. On the one SCID-non recon pig that remained healthy until the end of the study, there was only slightly increase in the concentration of $CD3^+$ T cells to 27 cells/ uL. The only WT pig had a concentration of 1756 cells/µL. From these data, we concluded that donor T lymphocytes had become engrafted in SCID recipients.

In addition, we did not see evidence of B cell engraftment (mean concentration <1 B cell/ uL) establishing that the preparation and sorting of thymocytes did not possess contaminating B cells from the donors. The population of NK cells in treated SCID was similar in concentration to the normal control, although the frequencies were slightly elevated in SCIDs compared to normal pigs (data not shown).

Immunophenotyping of $CD3^+$ T lymphocytes in peripheral blood at day 49 post adoptive transfer

Since there was no evidence of engraftment in the receptor SCID pigs on Experiment A, immunophenotyping was not performed on those animals.

For Experiment B, peripheral blood $CD3^+$ T cell subtype populations in all WT, SCID-non recon, and SCID-recon pigs were further characterized using multi-parameter flow

cytometry analysis. Results of the analysis are shown in Figure 5.4. The T cell subsets in SCID-recon piglets were comprised primarily of CD8+ single positive (SP) T cells (N=3, mean number = 30,248 cells/ uL blood, mean percentage = 36.75%; S.D.= 13.904) and $CD4^{+}CD8^{+}$ double positive (DP) T cells (N=3, mean number = 43461.6 cells/ uL blood, mean percentage = 56.80%; S.D.= 16.574), a subset that has been described as a memory T-helper population in pigs (Zuckermann *et al.* 1996). This is likely the result of "lymphopenia-induced proliferation", an homeostatic response of naïve T cells in which these cells differentiate and expand into $CD8^{+}$ T cells following T cell transfer in immunodeficient hosts (Suhr and Sprent, 2008, Hamilton *et al.* 2006, Johnson and Jameson, 2010). $CD4^{+}CD8^{+}$ double positive (DP) T cells are generally regarded as activated, or memory T helper cells in normal animals (Nascimbeni, *et al.* 2004, Buttlar *et al.* 2015); however, no signs of graft versus host disease were observed in reconstituted SCID pigs. Likely, this phenotype is a consequence of the lymphopenic environment, as adoptively transferred naïve T cells in murine SCID animals will typically display an activated phenotype until T cell homeostasis is achieved.

Also of note, the $CD4^{-}CD8^{-}$ double negative T cell population was greatly reduced in both SCID-non recon (mean = 110.7 cells/µl blood, mean percentage = 4.1%) and SCID-recon (mean = 971.12 cells/µl blood, mean percentage = 1.25%) animals, compared to the WT pigs (mean = 72522 cells/µl blood, mean percentage = 41.8%). These cells constitute a population of γδ T cells ($TCR1^{+}CD8^{-}$ subset of CD3+ T cells) that are generated from fetal liver in utero (Figure 5.4). Young pigs have a very prominent population of γδ T cells in peripheral blood, which decrease as they age (Gerner *et al.* 2009).

We also assessed the level of regulatory T cells (T regs, $CD3^{+}CD4^{+}CD25^{+}FoxP3^{+}$) in all animals, as this may be a population that modulates macrophage permissiveness to PRRSV

infection. As demonstrated in Figure 5.4, T regs ($FoxP3^{+}CD25^{hi}$) constituted 2.4% of $CD4^{+}CD3^{+}$ T cells in normal animals (mean number = 4214.4 cells/µl blood). In SCID-recon animals, adoptive transfer of thymocytes gave rise to a lower, but detectable T reg population with a mean percentage of 1.35% of $CD4^{+}CD3^{+}$ (mean number = 1114.4 cells/µl blood) in peripheral blood. The development of T cell subsets, especially T regs, following adoptive T cell transfer into SCID recipients is critical to establishing this reconstitution model as a means to evaluate the role of T cells and Tregs during PRRSV infection. These cells have been extensively reported to provide protection against autoimmunity and graft versus host disease in other lymphopenic models (Beres and Drobyski, 2013). In this study, we did not see evidence of graft-versus-host disease in any of our recipient SCIDs, although additional long-term engraftment studies will be required in order to evaluate where T cell reconstitution in this model will lead to chronic graft-versus-host disease.

Assessment of Lymphoid Tissues by Immunohistochemistry

Tissues were collected from normal, SCID, and thymocyte-treated SCID animals at day 49 post adoptive transfer, and submitted for pathological assessment. As demonstrated in Figure 8, elevated levels of tissue-resident CD3+ cells were detected by immunohistochemistry in reconstituted animals, when compared to untreated SCID piglets. While the level of T cells observed in thymocyte-treated SCIDs were somewhat lower from the normal control animal, this data clearly established the engraftment of CD3+ cells in a number of lymphoid tissues, and corroborated the flow cytometric data generated from peripheral blood.

Analysis of thymocytes

Tissues were collected from WT, SCID-recon, and SCID-non recon pigs at day 49 post adoptive transfer, and were subjected to microscopic examination by a certified veterinary pathologist. H&E staining of thymic tissue demonstrated increased numbers of thymocytes, in comparison to the SCID-non recon. In multiple areas, there were areas of cortico-medullary demarcation (Figure 5.5.A). Increased numbers of thymocytes in the cortex of SCID-recon was confirmed by a $CD3^+$ staining T cell populations (Figure 5.6A). The thymus of the SCID-non recon was very small and did not presented cortico-medullary demarcation, as described before (Ewen *et al.* 2014). Figure 5.6B demonstrates the lack of $CD79a^+$ B cells in thymus by immunohistochemistry.

Lymph nodes from SCID-recon pigs revealed aggregates of lymphocytes, which formed lymphoid-like structures (Figure 5.5.B). These lymphocytes were positive for T cell markers in immunohistochemistry (Figure 5.6.C). The lymph node of SCID-non recon revealed total absence of lymphoid follicles with germinal centers, as is usually observed in SCID animals. Very few foci of $CD79a^+$ B cells are identified in immunohistochemically stained slides from SCID-recon lymph node (Figure 5.6.D).

Figure 5.5.C illustrates ileal Peyer's patches in normal, SCID-non recon and SCID-recon pigs. As previously reported (Cino-Ozuna *et al.* 2013 and Ewen *et al.* 2014), SCID-non recon are devoid of Peyer's patches, and only sparse numbers of T cells could be detected throughout the tissue. In contrast, SCID-recon contained an obvious increase in the number thickness of the Peyer's patches due to the presence of markedly increased numbers of $CD3^+$ T cells distributed at the epithelial-lamina propria junction, and throughout the epithelial layer by immunohistochemistry (data not shown).

Immunohistochemical analysis of the spleen of SCID-recon also demonstrated the recruitment of $CD3^+$ T cells in areas reminiscent of periarteriole lymphoid sheaths observed in WT pigs (data not shown). This shows evidence of the engraftment of functional thymocyte precursors into the thymus, lymph node, Peyer's patches and spleen, with the formation of lymphoid follicular structures characteristics of the specific organ tissue. Engraftment of thymocytes into thymus would likely lead to long-term T cell reconstitution in reconstituted piglets. Additional long-term reconstitution studies would be necessary to determine long-term T cell engraftment, and to evaluate the presence of graft versus host reaction.

5.D. Conclusion

Engraftment of common porcine T cell subsets, including regulatory T cells, was achieved by the adoptive transfer of purified thymocytes from WT pigs into SLA-II matched SCID pigs. These results were assessed by immunohistochemical and flow cytometry-based techniques. We conclude that we have developed a new model to directly study the immunopathology of subsets of T lymphocytes as well as their interaction with macrophages. Furthermore, this model could be used to investigate the interaction of these cells during viral infections, such as with PRRSV or African swine fever virus (ASFV). The data that would be generated in this type of experiments may be useful to further characterize the role of T cells, and to understand the mechanisms of activation or suppression of macrophages, with potential for the development of more effective vaccines in the future.

5.D. References

1. Basel, M.T., Balivada, S., Beck, A.P., Kerrigan, M.A., Pyle, M.M., Wyatt, C.R., Rowland, R.R.R., Anderson, D.E., Troyer, D.L. (2012). Human xenografts are not rejected in a naturally occurring immunodeficient porcine line: a human tumor model in pigs. *Biores. Open Access* 1, 63–68.

2. Bell, T.G., Butler, K.L., Sill, H.B., Stickle, J.E., Ramos-Vara, J.A., Dark, M.S. (2002). Autosomal recessive severe combined immunodeficiency of Jack Russell Terriers. *J. Vet. Diagn. Invest.* 14, 194–204.

3. Blunt, T., Finnie, N.J., Taccioli, G.E., Smith, G.C.M., Demengeot, J., Gottlieb, J.M., Mizuta, R., Varghese, A.J., Alt, F.W., Jeggo, P.A., Jackson, S.P. (1995). Defective DNA-dependent protein kinase activity is linked to V(D)J recombination and DNA repair defects associated with the murine scid mutation. *Cell* 80, 813–823.

4. Cino-Ozuna, A.G., Rowland, R.R.R., Nietfeld, J.C., Kerrigan, M.A., Dekkers,J.C., Wyatt, C.R. (2013). Preliminary findings of a previously unrecognized porcine primary immunodeficiency disorder. *Vet. Pathol.* 50,144–146.

5. Crump, A.L., Grusby, M.J., Glimcher, L.H., and Cantor, H. (1993). hymocyte development in major histocompatibility complex- deficient mice: Evidence for stochastic commitment to the CD4 and CD8 lineages. *Proc. NAtl. Acad. Sci. USA* 90, 10739 -10743.

6. Danska, J.S., Holland, D.P., Mariathasan, S., Williams, K.M., Guidos, C.J. (1996). Biochemical and genetic defects in the DNA-dependent protein kinase in murine scid lymphocytes. *Mol. Cell. Biol.* 16, 5507–5517.

7. Ewen, C.L., Cino-Ozuna, A.G., He, H., Kerrigan, M.A., Dekker, J.C.M., Tuggle, C.K., Rowland, R.R.R., and Wyatt, C.R. (2014) Analysis of blood leukocytes in a naturally occurring immunodeficiency of pigs shows the defect is localized to B and T cells. *Veterinary Immunology and Immunopathology* 162, 174-179.

8. Hamilton, S.E., Wolkers, M.C., Schoenberger, S.P., and Jameson, S.C. (2006). The generation of protective memory-like CD8+ T cells during homeostatic proliferation requires CD4+ T cells. *Nature immunology*. 7(5):475–481.

9. Ho, C. S., J. K. Lunney, J. H. Lee, M. H. Franzo-Romain, G. W. Martens, R. R. Rowland, and D. M. Smith. (2010). Molecular characterization of swine leucocyte antigen class II genes in outbred pig populations. *Anim Genet* 41:428-432.

10. Ho, C. S., J. K. Lunney, M. H. Franzo-Romain, G. W. Martens, Y. J. Lee, J. H. Lee, M. Wysocki, R. R. Rowland, and D. M. Smith. (2009). Molecular characterization of swine leucocyte antigen class I genes in outbred pig populations. *Anim Genet* 40:468-478.

11. Ito, T., Y. Sendai, S. Yamazaki, M. Seki-Soma, K. Hirose, M. Watanabe, K. Fukawa, and H. Nakauchi. (2014). Generation of recombination activating gene-1-deficient neonatal piglets: a model of T and B cell deficient severe combined immune deficiency. *PLoS One* 9:e113833

12. Johnson, L. D. S. and Jameson, S. C. (2010). Self-specific CD8+ T cells maintain a semi-naïve state following lymphopenia-induced proliferation. *J. Immunol.* 184(10):5604-5611.

13. Mair, K. H., C. Sedlak, T. Kaser, A. Pasternak, B. Levast, W. Gerner, A. Saalmuller, A. Summerfield, V. Gerdts, H. L. Wilson, and F. Meurens. (2014). The porcine innate immune system: an update. *Dev Comp Immunol* 45:321-343.

14. Meek, K., Kienker, L., Dallas, C., Wang, W., Dark, M.J., Venta, P.J., Huie, M.L.,Hirschhorn, R., Bell, T. (2001). SCID in Jack Russell Terriers: a new animal model of DNA-PKcs deficiency. *J. Immunol.* 167, 142–2150.

15. Meurens, F., A. Summerfield, H. Nauwynck, L. Saif, and V. Gerdts. (2012). The pig: a model for human infectious diseases. *Trends Microbiol* 20:50-57.

16. Nascimbeni, M., Shin, E-C., Chiriboga, L., Kleiner, D.E., and Reherman, B. (2004). Peripheral CD4+CD8+ T cells are differentiated effector memory cells with antiviral functions. *Blood* 104 (2):478-486.

17. Notarangelo, L.D. (2010). Primary immunodeficiencies. *J. Allergy Clin. Immunol* 152 (2 Suppl. 2): S182-S194.

18. Surh, C.D. and Sprent, J. (2008). Homeostasis of Naive and Memory T Cells. *Immunity*. 29:848–862.

19. Suzuki, S., M. Iwamoto, Y. Saito, D. Fuchimoto, S. Sembon, M. Suzuki, S. Mikawa, M. Hashimoto, Y. Aoki, Y. Najima, S. Takagi, N. Suzuki, E. Suzuki, M. Kubo, J. Mimuro, Y. Kashiwakura, S. Madoiwa, Y. Sakata, A. C. Perry, F. Ishikawa, and A. Onishi. (2012). Il2rg gene-targeted severe combined immunodeficiency pigs. *Cell Stem Cell* 10:753-758.

20. Von Buttlar, H., Bismarck, D., and Alber, G. (2015). Peripheral canine CD4+CD8+ double-positive T cells – unique amongst others. *Vet. Immunol. Immunopathol.*168 (3-4):169-175.

21. Waide, E.H., Dekkers, J.C.M., Ross, J.W., Rowland, R.R.R., Wyatt, C.R. Ewen, C.L., Evans, A.B., Thekkoot, D.M., Boddicker, N.J., Serão, N.V.L., Ellinwood, N.M., and Tuggle, C.K. (2015). Not All SCID Pigs Are Created Equally: Two Independent Mutations in the Artemis Gene Cause SCID in Pigs. *J. Immunol.* 195:3171-3179.

22. Zuckermann, F. A., and R. J. Husmann. (1996). Functional and phenotypic analysis of porcine peripheral blood CD4/CD8 double-positive T cells. *Immunology* 87:500-512.

23. Gerner, W., T. Kaser, and A. Saalmuller. (2009). Porcine T lymphocytes and NK cells--an update. *Dev Comp Immunol* 33:310-320.

24. Beres, A.J. and Drobyski, W.R. (2013). The Role of Regulatory T Cells in the Biology of Graft Versus Host Disease. *Front Immunol*. 4(163):1-9.

Tables and Figures

Figure 5.1 Outline of the projects

Major procedures in Experiment A (mature T cell transfer) are depicted in the top gray lines at the top. Procedures on experiment B (thymocyte transfer) are depicted in the purple lines at the bottom.

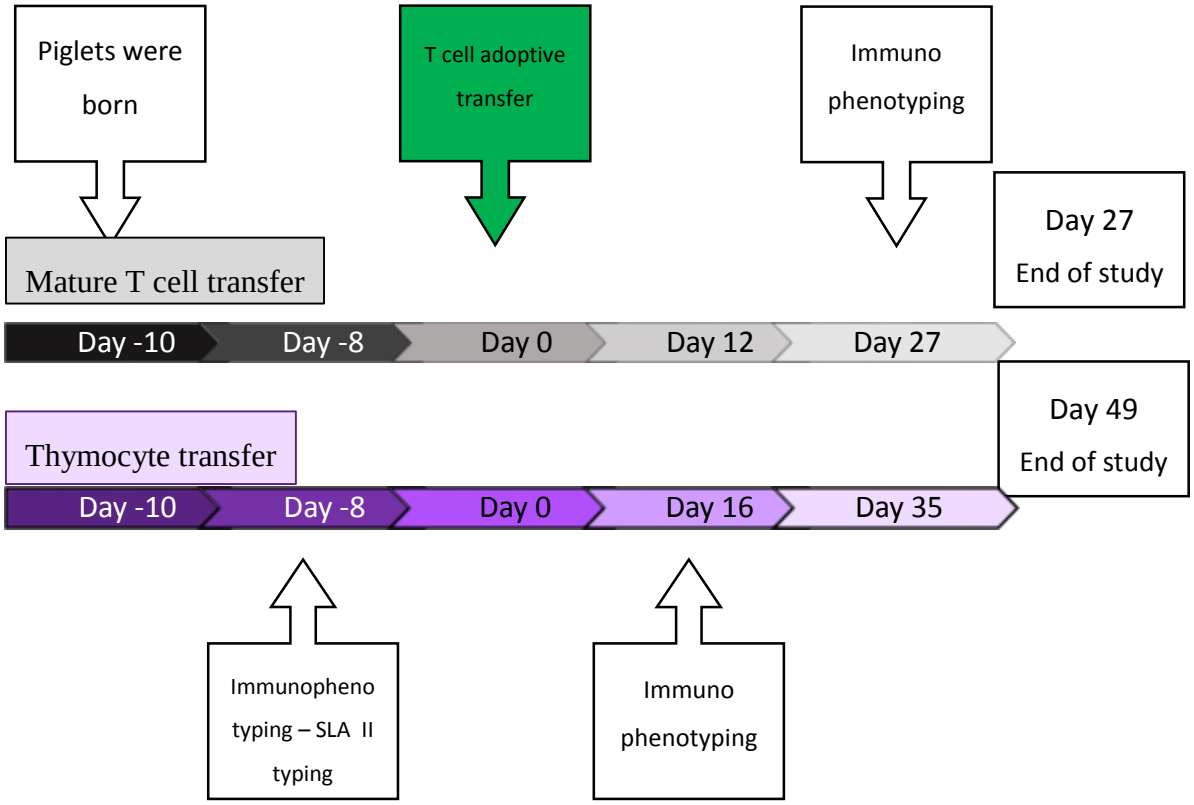

Figure 5.2 Number of CD3+ T lymphocytes and CD21+ B lymphocytes in peripheral blood of WT and SCID pigs at three days after birth.

Numbers represent concentration of cells / μL of whole blood.

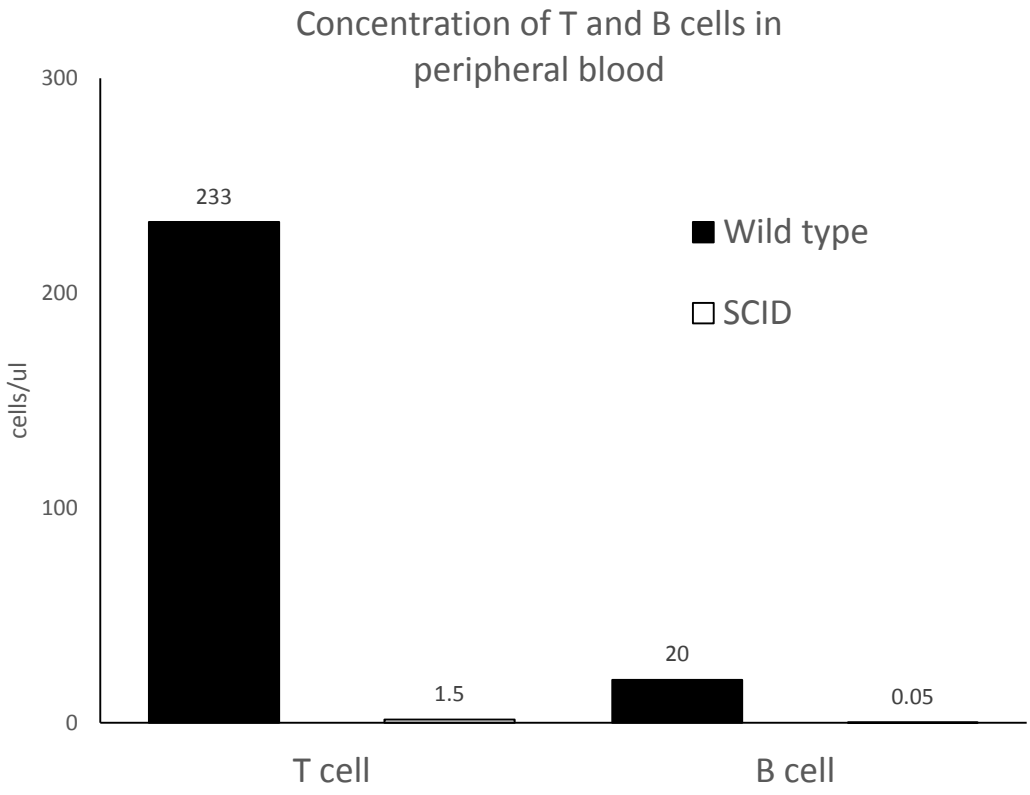

Figure 5.3 Experiment B: CD3+ T cell population in peripheral blood in wild type (WT), non-reconstituted SCID (SCID-Non recon) pigs and reconstituted (SCID-Recon) at days -9, +16, +35, and +49 post adoptive transfer.

Representative histogram plots from each group showing the frequencies of $CD3^+$ T cells (dark black lines) in comparison with the isotype control (gray line). Cell counts are indicated on the y-axis.

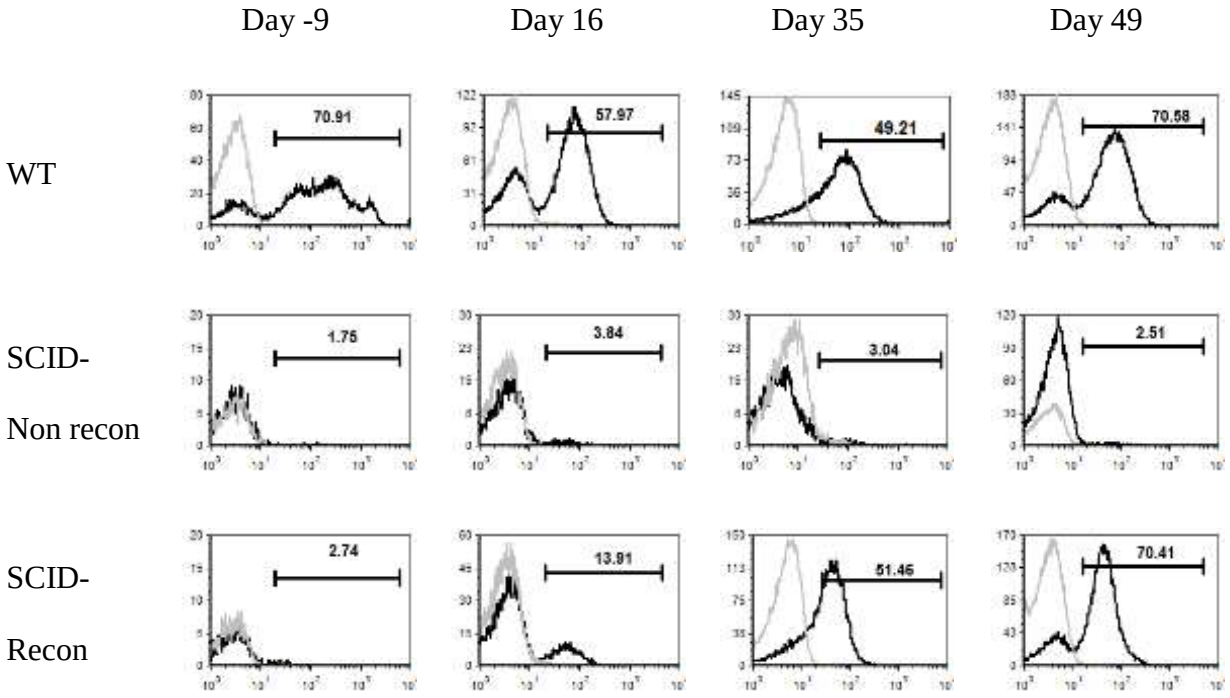

Figure 5.4 CD3+ T cell subset population in peripheral blood in wild type, reconstituted (SCID-Recon) and non-reconstituted SCID (SCID-Non recon) pigs at day 49 post adoptive transfer.

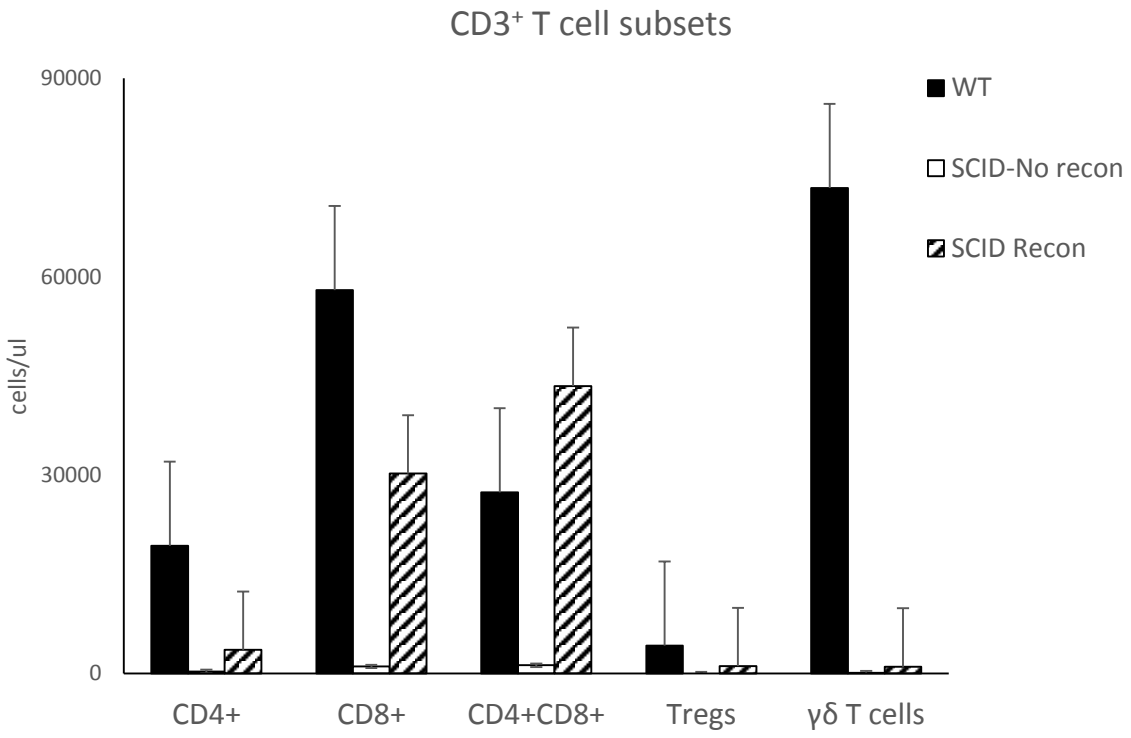

Figure 5.5 Histology of primary and secondary lymphoid tissues at 49 days of adoptive transfer of T lymphocytes.

Panel A shows representative microscopic findings of thymus, Panel B of lymph nodes, and Panel C of Peyer Patches from wild type, no transfer SCID, and T cell-transfer SCID pigs. T cell transfer SCID had increased T cell population in both thymus and lymph nodes, with delimitation of cortex and medulla of the thymus (arrow heads) and formation of lymphoid follicles in the lymph node (arrows) and Peyer patches, whereas thymus and lymph node in non transfer-SCID remains hypoplastic. All images are at the same scale (4X).

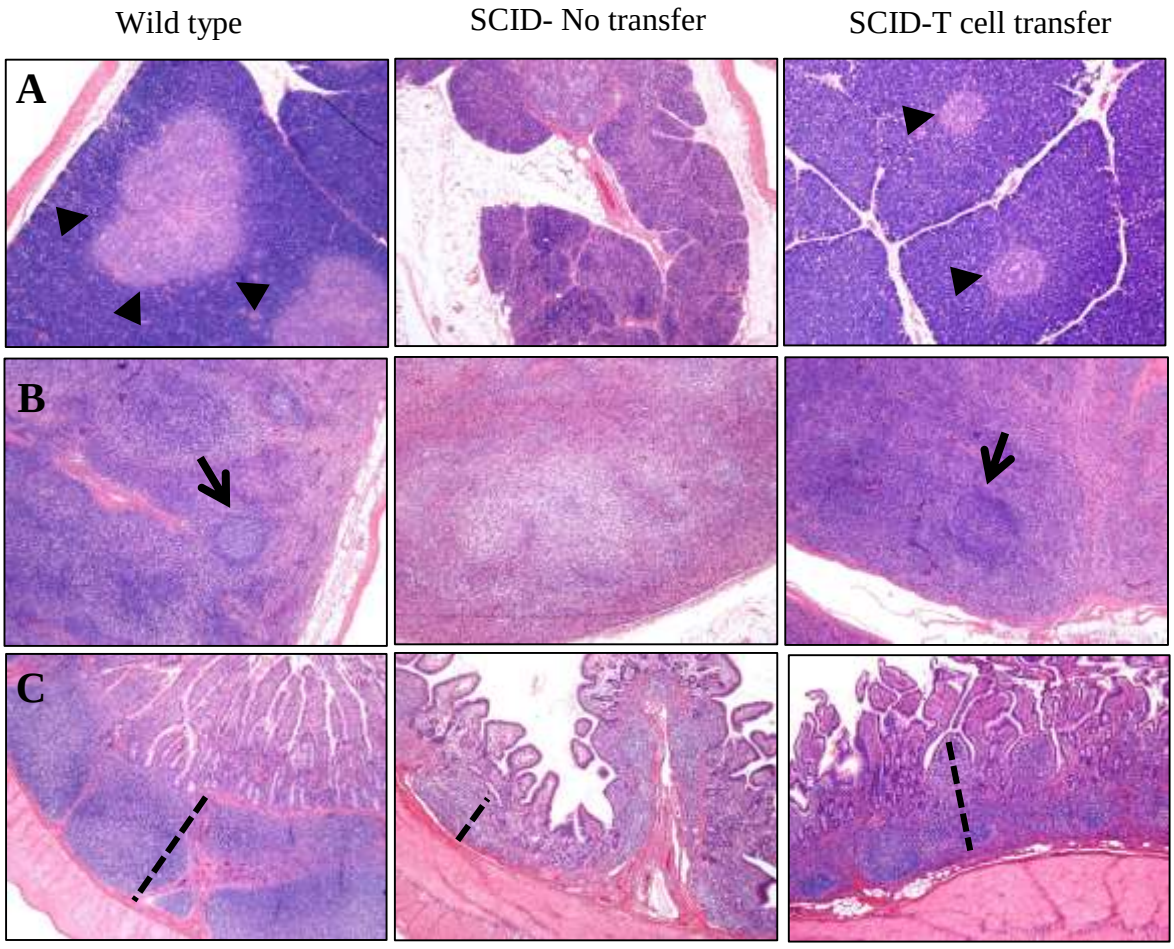

Figure 5.6 Immunohistochemistry for T and B cells at 49 days after T cell reconstitution.
Panel A shows staining of T lymphocytes with T cell marker CD3. Arrow heads indicate the delimitation between cortex and medulla in both wild type and SCID-T cell transfer, while this delimitation is absent in SCID-no transfer pig. Panel B shows the same areas stained with B cell marker CD79α with pale brown positive cells in the medulla (arrow heads). Note the lack of cortico-medullary delimitation on SCID-no transfer pig. Panel C and D shows lymph node staining with T and B cell markers CD3 and CD79α, respectively. Arrows point to the lymphoid follicles with germinal centers, which are absent in SCID-non transfer.

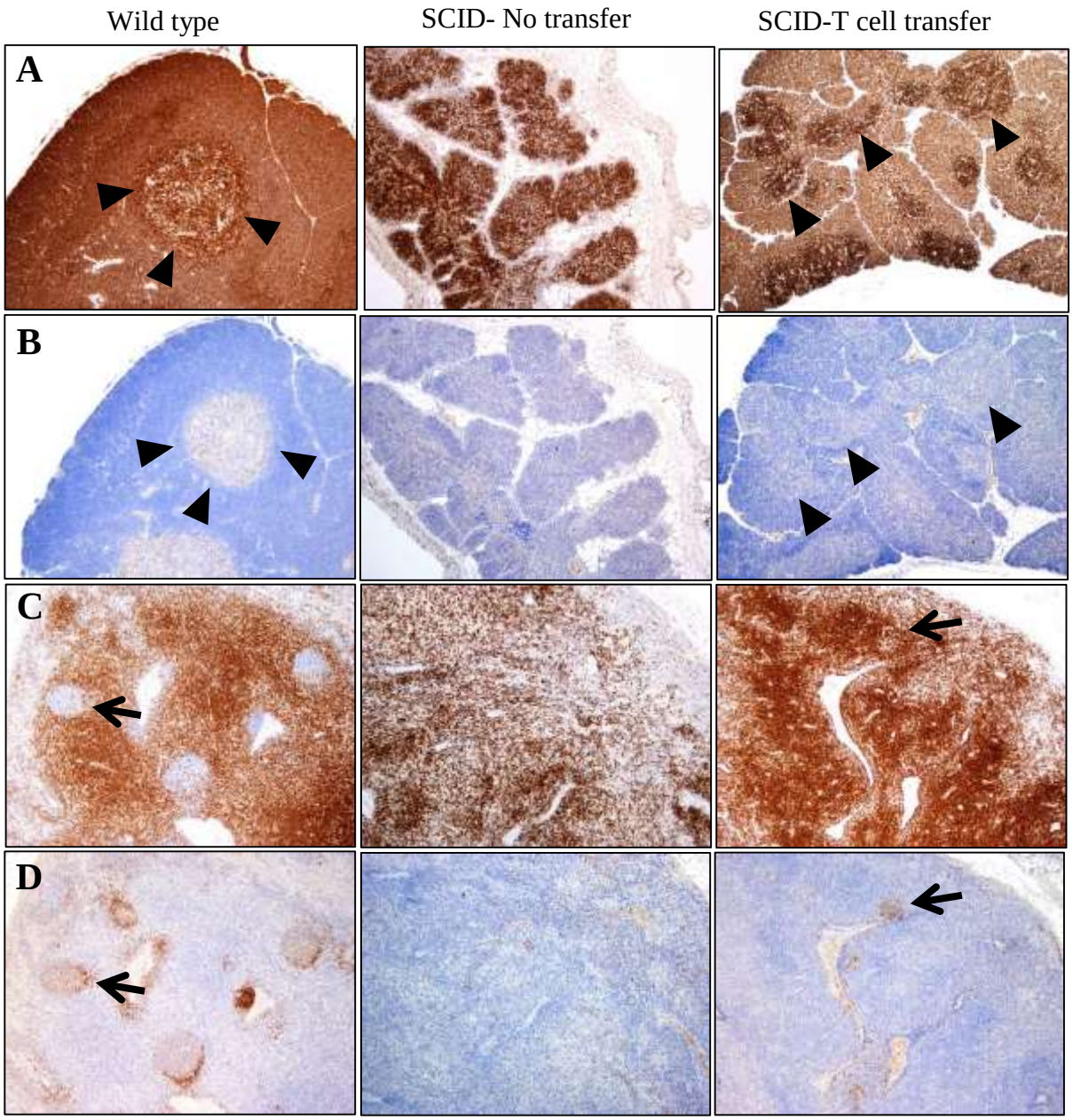

Table 5.1 SLA II-matching and immunophenotyping of pigs on experiments A and B.

Experiment A

Pig ID	Phenotype	Sex	Donor/Recipient
A1	WT	F	-
A2	WT	F	Donor 1
A3	WT	F	Donor 2
A4	WT	M	-
A5	SCID	M	Recipient 1
A6	SCID	M	Recipient 2
A7	SCID	M	-
A8	WT	M	-

Experiment B

Pig ID	Phenotype	Sex	Donor/Recipient
B1	WT	M	-
B3	WT	M	Donor 1
B4	SCID	F	Recipient 2
B5	SCID	M	-
B6	SCID	M	-
B7	SCID	M	Recipient 1
B8	WT	M	Donor 2
B9	SCID	M	-
B10	WT	M	Donor 3
B11	SCID	M	Recipient 4
B12	WT	F	Donor 4
B13	SCID	M	-
B14	SCID	M	Recipient 3

Table 5.2 Primary and secondary antibodies used for flow cytometry on PBMCs.

Blood leukocytes

Primary antibody	**Fluorochrome**	**Clone**
CD3ε	R-phycoerythrin (R-PE)	PPT3
CD4	Fluorescein isothiocyanate (FITC)	74-12-4
CD8α	Phycoerythrin (P-Cy5E)	76-2-11
CD14	Pacific Blue (PB)	TÜK4
CD16	R-PE	G7
CD21	Allophycocyanin (APC)	B-ly4
CD25	No fluorochrome (IgG1)	PGBL25A
γδ T cell	No fluorochrome (IgG1)	PGBL22A
FoxP3	R-phycoerythrin-Cyanine 7 (PE/Cy®7)	FJK-16s
Secondary antibody	**Fluorochrome**	**Clone**
IgG1	Brilliant violet 421 (BV421)	RMG1-1

Table 5.3 Primary and secondary antibodies used for flow cytometry on thymocytes.

Thymocytes

Primary antibody	**Fluorochrome**	**Clone**
CD3ε	R-phycoerythrin (R-PE)	PPT3
CD1	Biotin (BIOT)	76-7-4
CD4	Fluorescein isothiocyanate (FITC)	74-12-4
CD8α	Phycoerythrin (P-Cy5E)	76-2-11
CD44	R-phycoerythrin-Cyanine 7 (PE/Cy®7)	IM7
TCR1-N4	VMRD	PGBL22A
CD21	Allophycocyanin (APC)	B-ly4
CD25	--(Isotype IgG1)	PGBL25A
γδ T cell	--(Isotype IgG1)	PGBL22A
FoxP3	R-phycoerythrin-Cyanine 7 (PE/Cy®7)	FJK-16s
Secondary antibody	**Fluorochrome**	**Clone**
IgG1	Brilliant violet 421 (BV421)	RMG1-1

Chapter 6 - Conclusions and future perspectives

The value of pigs as a biomedical model for animal and human diseases has rapidly grown in the past few years. This is because of the remarkable similarities between swine species and humans, including anatomic, genetic, and physiologic features (Meurens *et al* 2012). The murine SCID animal models had been the gold standard for studies of immunology, cancer, and transplantation models. However, it is known that murine species do not always extrapolate accurately the data when evaluating human or other animal species. Therefore, there is a growing need for the development of a immunodeficiency model in an alternative species, and swine is a desired target. The recent publications of genetically engineered SCID pigs demonstrate the raising hope and the focus of the industry in the development of a porcine SCID model (Huang *et al* 2014 and Lee *et al.* 2014). Therefore, the description of a line of pigs with naturally occurring SCID and the associated mutations in *Artemis* gene is, at minimum, very exciting (Weide *et al.* 2015) and promising. These SCID pigs share the same characteristics as other animals species that develop SCID phenotype, which include lack of B and T lymphocytes leading to lymphopenia, lymphoid hypoplasia, and inability to mount an antibody response. Our SCID pigs have normal numbers of granulocytes, monocytes, and NK cells in circulation (Cino-Ozuna *et al* 2013 and Ewen *et al.* 2014). However, based on the fact that NK cells showed incapable of responding to xerograph transplantation (Basel *et al* 2012), although they remain in normal numbers in circulation, we hypothesize that NK cells functionality is absent. A further investigation into this topic is necessary and would have applications in the understanding of the role of NK cells in cancer immunology.

We have shown that our porcine SCID model has the ability to growth human xenotransplanted cancer cells (Basel *et al* 2012). Successful transplantation of a variety of normal and malignant human cell populations and tissues is another application of our SCID pig model. The development of such a model would be useful for the study of potential molecular targets for vaccination and cancer development, as well as the development of targets and evaluation of their efficacy and safety, without the distraction that sometimes represents the immune response of the host to the cancer cells.

Another interesting aspect of this natural model of SCID in pigs is the presence of low numbers of $CD3^+$ T lymphocytes in circularion and γδ T lymphocytes in the Peyer's Patches in some affected animals. Although immunoglobulin (Ig) was not detected in circulation in these pigs, the presence of circulating T lymphocytes is consistent with the "leaky SCID" mice phenotype (Bosna *et al*. 1988). Leaky SCID was only described in C.B.-17 to date. These animals are characterized by low numbers of T lymphocytes and very low levels of antibodies in circulation. It would be interesting to further investigate genotype differences between the "leaky SCID" pigs and true SCID pigs. In addition, further investigation and characterization of γδ T lymphocytes on these pigs may provide answers as to the molecular factors that are involved in the development and functionality of this poorly understood subset of lymphocytes.

Using an alternative murine SCID model system, in which mature or immature lymphocytes can be adoptively transferred and engrafted into SCID animals, has been sought for some time. Most typically, the reconstitution of immunodeficient animal species and humans is develop by transfer of bone marrow cells from a matched donor. The disadvantages of this technique, however, rely on the lack of phenotypic specificity and possibility of contamination with other cell types. In our experiments, we showed that successful reconstitution of purified

lymphocytes is possible in our porcine SCID model. The ability to engraft a specific phenotype of lymphocytes or other immune cells into SCID pigs, provides the opportunity to further investigate the immune response expansion, maturation, and activation.

The gap in knowledge in the immunopathogenesis of catastrophic viral diseases in porcine species, such as with PRRSV, ASFV, CSFV, is vast. Therefore, the need for a porcine model that would allow the study of the immune response to this devastating diseases is indispensable. The ability to reconstitute our SCID pigs with specific lineage of immune cells opens the opportunity to study the immune system response to these and many other viral diseases.

A future perspective of our reconstituted porcine SCID model would be the development of specific viral disease models, such as with ASFV. African swine fever virus (ASFV) causes a highly contagious disease in domestic and wild swine and is considered one of the most relevant viral infections of swine throughout the world. ASF is present in eastern and central European countries and Sardinia and in numerous African countries, but it's absent in the Unites States. For this reason, models of infection to study and understand ASFV infection in pigs to prevent its entrance to the United States are imperative.

Similar to PRRSV, ASFV targets cells of the mononuclear phagocytic lineage, including macrophages and monocytes. (Malmquist and Hay, 1960, Gomez-Villamandos *et al.* 1995) and share the same cellular receptor as PRRSV, CD163.

PRRSV infection in our porcine SCID model revealed that alveolar macrophages are permissive to PRRSV entry and replication. Furthermore, our porcine SCID model revealed that PAMs markers CD172, CD163, and MHC class II are similar among SCID and wild type

littermates, indicating the normal expression of these molecules in the SCID pigs. Therefore, it is expected that SCID pig PAMs would be permissive to infection of ASFV.

Cell-mediated immune response is essential for the control of virus diseases. However, it is sometimes detrimental to the individual, as the overwhelming secretion of cytokines from effector T cells can lead to recruitment of more inflammatory cells and tissue damage. (Barry and Bleackeley, 2002). In viral infections, following recruitment of effector T cells and other cells, such as NK cells and NKT cells to the site of inflammation, these cells secrete IFN-γ, a cytokine that enhances secretion of proinflammatory cytokines and chemokines, and antimicrobial activity of macrophages. One example of such a detrimental response is infection with AFSV. Exposure of modified isolates of ASFV induces production of ASFV-specific IFN-γ, which results in protection against the virus. (Takamatsu *et al*. 2013). Therefore, the response of our porcine SCID reconstituted model to ASFV infection using specific $CD8^+$ T cells or other purified phenotypes of lymphocytes is a potential use of the SCID pigs. Furthermore, there is a need for a better understanding of the stimulation and enhancement of anti-viral macrophagic functions, with the purpose of the development of more accurate methods of therapy and prevention of disease through the development of vaccines.

Finally, our porcine SCID model could be used for the study of the immune dysregulation observed with PRRSV infection. Following, are some possible applications of our porcine SCID model of PRRSV infection.

- Characterization of PRRSV-related adaptive immune response in SCID pigs after adoptive transfer of T cells: SCID pigs infected with PRRSV virus fail to develop characteristic lesions, proving that T cells play a crucial role in the immunopathogenesis of the disease. Infection of PRRSV after T cell adoptive

transfer of SCID pigs will help not only in the understanding of the mechanisms of cell immunity, but also elucidate the role of the T lymphocytes during immune evasion of PRRSV. Extensive studies have demonstrated that there is a delayed and transient T cell response following PRRSV infection, thus analysis of T cell response at different set times of viremia would be important in order to further understand this mechanism of delayed response.

- Immunologic anergy: Very few porcine studies focused in the immune evasion of PRRSV through the induction of anergy in T cells. Anergy is by definition a state of unresponsiveness induced when T cell receptor (TCR) is stimulated by an antigen but there is negative "second signal" induced by the antigen presenting cells. The second signal is induced by various co-stimulatory receptors such as CD28 and CTLA-4 that bind CD80 and CD86 (B7-1 and B7-1, respectively). CD28 is constitutively expressed on native and activated CD4 and CD8 positive T cells. CTLA-4 is expressed on activated T cells and plays a negative regulatory role in T cell response. CD80 and CD86 are induced on antigen presenting cells (APC) with their activation. Multiple studies in human, macaque, and mouse retroviruses demonstrated the induction of anergy in T cells as a mechanism of viral immune dysregulation. CTLA-4 expression on T cells from reconstituted SCID pigs would help further understanding the role of this molecule during PRRSV immune dysregulation.

- Inappropriate activation of T regs: Numerous studies revealed that regulatory T cells (T regs) are induced after infection with PRRSV and other viruses, such as human and murine cytomegalovirus and retroviruses. In the T cell reconstituted SCID pigs, measuring the numbers of T regulatory cells and correlating their numbers with PRRSV viral load in tissues, such as lung and lymph nodes, would be very important to study the role of T regs in immune dysregulation. Markers for T regs include CD4, CD3, Fox-P3 and CD25 and would be used to identify these cells.

In conclusion, our porcine SCID model has multiple applications in different fields, such as cancer research, autoimmune disase, and immunopathogenesis and dysregulation of viral diseases, especially devastating porcine ones such as PRRSV and ASFV.

5.A. References

1. Barry, M., Bleackley, R.C. (2002). Cytotoxic T lymphocytes: all roads lead to death. *Nature Review Immunology* 2 401–409.

2. Basel, M.T., Balivada, S., Beck, A.P., Kerrigan, M.A., Pyle, M.M., Wyatt, C.R., Rowland, R.R.R., Anderson, D.E., Troyer, D.L. (2012). Human xenografts are not rejected in a naturally occurring immunodeficient porcine line: a human tumor model in pigs. *Biores. Open Access* 1, 63–68.

3. Bosma GC, Fried M, Custer RP, et al. (1988). T Evidence of functional lymphocytes in some (leaky) scid mice. *J Experim Med*. 167(3):1016-1033.

4. Cino-Ozuna, A.G., Rowland, R.R.R., Nietfeld, J.C., Kerrigan, M.A., Dekkers,J.C., Wyatt, C.R. (2013). Preliminary findings of a previously unrecognized porcine primary immunodeficiency disorder. *Vet. Pathol.* 50,144–146.

5. Ewen C. L., Cino-Ozuna A. G., He H., Kerrigan M. A., Dekker J. C. M., Tuggle C. K., Rowland R. R. R., and Wyatt C. R. (2014) Analysis of blood leukocytes in a naturally occurring immunodeficiency of pigs shows the defect is localized to B and T cells. *Veterinary Immunology and Immunopathology* 162, 174-179.

6. Gomez-Villamandos, J.C., Herv,as J., Mendez, A., Carrasco, L., Martın de las Mulas, J. (1995). Experimental African swine fever: apoptosis of lymphocytes and virus replication in in other cells. *Journal of General Virology* 76, 2399-2405.

7. Huang, J., Guo, X., Fan, N., Son, J., Zhao, B., Ouyang, Z., Liu, Z., Zhao, Y., Yan, Q., Yi, X., Schambach, A., Frampton, J., Esteban, M.A., Yang, D., Yang, H., and Lai, L. (2014). RAG1/2 knockout pigs with severe combined immunodeficiency. J Immunol. Aug 1;193(3):1496-503

8. Lee, K., Kwon, D.N., Ezashi, T., Choi, Y.J., Park, C., Ericsson, A.C., Brown, A.N., Samuel, M.S., Park, K.W., Walters, E.M., Kim, D.Y., Kim, J.H., Franklin, C.L., Murphy, C.N., Roberts, R.M., Prather, R.S., Kim, J.H. (2014). Engraftment of human iPS cells and allogeneic porcine cells into pigs with inactivated RAG2 and accompanying severe combined immunodeficiency. Proc Natl Acad Sci USA. May 20;111(20):7260-7265

9. Malmquist, W.A., Hay, D. (1960). Hemadsorption and cytopathic effect produced by African swine fever virus in swine bone marrow and buffy coat cultures. *American Journal of Veterinary Research* 21,104-108.

10. Meurens, F.A., Summerfield, A., Nauwynck, H., Saif, L., and Gerdts, V. (2012). The pig: a model for human infectious diseases. Trends Microbiol. 2012 Jan;20(1):50-57.

11. Takamatsu, H.-H., Denyera, M.S., Lacasta, A., Stirling, C.M.A., Argilaguet, J.M., Nethertona, C.L., Ouraa, C.A.L. Martins, C., and Rodríguez, F. (2013). Cellular immunity in ASFV responses. *Virus Research* 173,110– 121.

12. Waide, E.H., Dekkers, J.C.M., Ross, J.W., Rowland, R.R.R., Wyatt, C.R. Ewen, C.L., Evans, A.B., Thekkoot, D.M., Boddicker, N.J., Serão, N.V.L., Ellinwood, N.M., and Tuggle, C.K. (2015). Not All SCID Pigs Are Created Equally: Two Independent Mutations in the Artemis Gene Cause SCID in Pigs. *J. Immunol.* 195:3171-3179.